HHS Public Access

Author manuscript

*Neuropharmacology*. Author manuscript; available in PMC 2017 June 16.

Published in final edited form as:

*Neuropharmacology*. 2016 December ; 111: 142–159. doi:10.1016/j.neuropharm.2016.09.001.

# TSPO activation modulates the effects of high pressure in a rat *ex vivo* glaucoma model

**Makoto Ishikawa**[1], **Takeshi Yoshitomi**[1], **Douglas F. Covey**[2,3], **Charles F. Zorumski**[3,4,5], and **Yukitoshi Izumi**[3,4,5]

[1]Department of Ophthalmology, Akita Graduate University School of Medicine, Akita, Japan

[2]Department of Developmental Biology, Washington University School of Medicine, St. Louis, M.O, USA

[3]Taylor Family Institute for Innovative Psychiatric Research, Washington University School of Medicine, St. Louis, M.O, USA

[4]Center for Brain Research in Mood Disorders, Washington University School of Medicine, St. Louis, M.O, USA

[5]Department of Psychiatry, Washington University School of Medicine, St. Louis, M.O, USA

## Abstract

We previously reported that elevated pressure induces axonal swelling and facilitates the synthesis of the neurosteroid, allopregnanolone (AlloP), in the *ex vivo* rat retina. Exogenously applied AlloP attenuates the axonal swelling, suggesting that the neurosteroid plays a neuroprotective role against glaucomatous pressure-induced injuries, although mechanisms underlying neurosteroidogenesis have not been clarified. The aim of this study was to determine whether AlloP synthesis involves activation of translocator protein 18 kD (TSPO) and whether TSPO modulates pressure-induced retinal injury. *Ex vivo* rat retinas were exposed to various pressures (10, 35, or 75 mmHg) for 24 hours. Expression of TSPO, 5α-reductase (5aRD), and AlloP was examined by quantitative real-time RT-PCR, ELISA, immunohistochemistry, and LC-MS/MS. We also examined the effects of TSPO ligands on AlloP synthesis and retinal damage. In this acute model, quantitative real-time RT-PCR and ELISA analyses revealed that elevated pressure facilitated TSPO expression. Similarly, these methods also detected enhanced 5aRD (mostly type II), which was observed in retinal ganglion cells (RGC) and the inner nuclear layer (INL). Atriol, a TSPO antagonist, suppressed pressure mediated AlloP synthesis and induced more severe histological changes in the inner retina when combined with elevated pressure. PK11195, a TSPO ligand that facilitates AlloP synthesis by itself, remarkably diminished pressure-mediated retinal degeneration. These results suggest that AlloP synthesis is induced by sequential activation of TSPO and 5aRD in an *ex vivo* glaucoma model, and that TSPO agonists may serve as potential therapeutic agents for the prevention of pressure-induced retinal damage.

Corresponding Author: Makoto Ishikawa, M.D. & Ph.D., Department of Ophthalmology, Akita Graduate University School of Medicine, 1-1-1 Hondo, Akita 010-8543, Japan, TEL: +81-18-834-1111, FAX: +81-18-836-2621, mako@med.akita-u.ac.jp.

**A conflict-of-interest statement:** CFZ serves on the Scientific Advisory Board of Sage Therapeutics. CFZ and DFC own stock in Sage Therapeutics. The other authors have no financial conflicts of interest.

**Keywords**

Neurosteroid; allopregnanolone; TSPO; 5α-reductase; glaucoma; neuroprotection

## 1. Introduction

Glaucoma is a leading cause of irreversible blindness (Pascolini and Mariotti, 2012; Tham et al., 2014). Among types of glaucoma, acute angle closure attacks (AAC) are an ophthalmic emergency and can lead to blindness (Aung et al., 2001). AAC involves a sudden rise in intraocular pressure (IOP) that can reach 80 mmHg (Ritch, 2000). If treatment is delayed, sustained IOP elevation damages retinal ganglion cells (RGC), and leads to severe visual disturbances (Lowe, 1973). However, the pathogenesis underlying RGC damage in AAC remains unclear, although glutamate excitotoxicity likely contributes to RGC death (Diekmann and Fischer, 2013; Louzada-Junior et al., 1992; Neal et al., 1994; Harada et al., 2007; Seki and Lipton, 2008). Glutamate is the most prevalent neurotransmitter in the retina (Thoreson and Witkovsky, 1999; Massey and Miller, 1987; Massey and Miller, 1990). When glutamate is in excess, it can become toxic to retinal neurons by overstimulation of glutamate receptors (Lucas and Newhouse, 1957; Olney, 1982).

Recently, we developed a new experimental model of AAC using an *ex vivo* rat retinal preparation to examine the effects of elevated hydrostatic pressure on retinal morphology and glutamate metabolism (Ishikawa et al., 2010, 2011). In this model, high pressure (75 mm Hg) induces axonal swelling in the nerve fiber layer (Ishikawa et al., 2010), accompanied by impaired glial glutamate transporters and metabolism (Ishikawa et al., 2011).

Gamma-aminobutyric acid (GABA) is an inhibitory neurotransmitter used by horizontal and amacrine cells in the lateral retinal pathway to modulate outer and inner synaptic layers (Kalloniatis and Tomisich, 1999; Yang, 2004). Although data indicate a role for glutamate in glaucoma (Naskar et al., 2000; Martin et al., 2002; Moreno et al., 2005; Nucci et al., 2005), the role of GABA has been less thoroughly investigated (Bailey et al., 2014), and prior work indicates that the balance between glutamate and GABA is important for maintaining retinal function (Kishida and Naka, 1968). However, there are only a few reports describing significant dysfunction of the GABAergic system in glaucomatous retinas (Bailey et al., 2014; Kishida and Naka, 1968; Moreno et al., 2008).

Allopregnanolone (AlloP) is a neurosteroid that can be locally synthesized in the central nervous system in response to stressful events. In the retina, AlloP is synthesized in response to pressure elevation (Ishikawa et al., 2014), and exerts neuroprotective effects via $GABA_A$ receptors in the *ex vivo* glaucoma model (Ishikawa et al., 2014). How acute stress promotes neurosteroid production is not certain.

In the brain, neurosteroids are generated from cholesterol by a series of steps that include shuttling of cholesterol to the inner mitochondrial membrane by translocator protein 18 kDa (TSPO) and conversion to pregnenolone by CYP11A1, a P450 side-chain cleavage enzyme (Weir et al., 2004; Belelli and Lambert, 2005; Rone et al., 2009; Gunn et al., 2011).

Pregnenolone exits the mitochondria and is converted to neurosteroids including AlloP. A major pathway involves the conversion of pregnenolone to AlloP by the sequential actions of 3β-hydroxysteroid dehydrogenase, 5α-reductase (5aRD) and 3α-hydroxysteroid dehydrogenase (Fig. 1a) (Belelli and Lambert, 2005; Rone et al., 2009). The translocation of cholesterol to the inner mitochondrial membrane by TSPO (Rupprecht et al., 2010) and the catalytic reaction by 5aRD (Dong et al., 2001; Agis-Balboa et al., 2007) in the endoplasmic reticulum membrane are considered rate limiting steps. Because elevated pressure enhances AlloP synthesis, we hypothesized that TSPO induction followed by 5aRD is required for AlloP synthesis when retinas are exposed to high pressure. In the present study, we tested this hypothesis by determining effects of pressure elevation on the expression of TSPO and 5aRD in an *ex vivo* glaucoma model. Moreover, we demonstrate that activation of TSPO is a key step in regulating retinal toxicity and that a TSPO antagonist promotes retinal excitotoxicity, while TSPO activation exerts neuroprotective effects via AlloP production.

## 2. Material and methods

Protocols for animal use were approved by the Akita University Animal Studies Committee in accordance with the guidelines of the Policies on the Use of Animals and Humans in Neuroscience Research.

### 2.1. Rat *ex vivo* Eyecup Preparation

Rat *ex vivo* eyecups were prepared from 28–32 day old male Sprague-Dawley rats (Charles River Laboratories International Inc., Wilmington, MA) as previously published (Ishikawa et al., 2010, 2011). The anterior half of the enucleated eyes was carefully removed to make eyecup preparations. Eyecups were placed at the bottom of a 100 ml glass beaker filled with aCSF (artificial cerebrospinal fluid) containing (in mM): 124 NaCl, 5 KCl, 2 $MgSO_4$, 2 $CaCl_2$, 1.25 $NaH_2PO_4$, 22 $NaHCO_3$, and 10 glucose, and incubated at 30°C for 24 hours using a closed pressure-loading system (Fig. 1b). pH was maintained at 7.35 to 7.40. In the closed-pressure system, a glass beaker with the eyecup was placed at the bottom of an acrylic pressure chamber (2,000 ml volume). A 95% $O_2$-5% $CO_2$ gas mixture was delivered through disposable plastic tubing with an infusion valve and a control dial on the lid of the pressure chamber and an air filter (Cat#SLGP033RS, Merk Millipore, Billerica, MA). The plastic tubing delivering the gas terminated 1 cm above the bottom of the beaker.

Acutely prepared eyecups were incubated in gassed aCSF for at least 1 h at 30°C before pressure loading. In some experiments, (3β,17β)-androst-5ene-3,17,19-triol (atriol) (1 μM), dizocilpine (MK801) (1 μM), AlloP (1 μM), isoquinoline carboxamide (PK11195) (50 μM) and dutasteride (1 μM) were dissolved in aCSF at the time of experiment and administered by bath perfusion. Eyecup preparations were treated with these drugs for 1 h at 30°C before pressure loading. For pressure loading, the 95% $O_2$-5% $CO_2$ gas mixture was infused until the pressure reading given by a manometer reached the appropriate level. The pressure was then locked by adjusting the control dial of the effusion valve, and monitored continuously for 24 h at 30°C. After maintaining the chamber at the set pressure (10, 35, 75 mmHg) for the indicated time, the pressure inside the chamber was carefully decreased by opening the effusion valve.

### 2.2. Quantitative real-time RT–PCR

We quantified *tspo* and *srd5a* mRNA expression in pressure-loaded eyecups incubated at 10, 35, and 75 mmHg for 24 h. At the end of each experiment, the retina of the empty eyecup was sampled, and immersed in RNAlater solution (Qiagen, Hilden, Germany), and frozen at −80°C. Total RNA was extracted by using RNeasy kit (Qiagen) from the retinal samples and used for cDNA synthesis. Aliquots (1 μg) of total RNA were reverse transcribed into first-strand cDNA by using a PrimeScrip® RT reagent kit (Takara Bio Inc. Shiga, Japan) and a thermal cycler (Takara PCR Thermal Cycler MP, Takara). Real-time reverse transcription (RT)–PCR reaction was carried out with a Thermal Cycler Dice® Real Time System (Takara). According to the manufacturer's instructions, the RT-PCR reaction was conducted in 25 μl of reaction buffer containing 12.5 μl SYBR® Premix Ex Taq II (Takara Bio Inc), 1 μl of 10 μM forward and reverse primers, 2 μl cDNA and 9.5 μl water. The RNA expression levels were normalized to the level of *gapdh* expression. Table 1 summarizes the primers used in the present study. The primers were designed using the Perfect Real Time® Support System (Takara). Quantitative real-time RT–PCR curves were analyzed by the crossing-point standard curve method.

In the present study, six independent experiments were performed for each condition. All PCR reactions were repeated in duplicate, and the average values were used for statistical analysis. The RNA expression levels were normalized to *gapdh* expression. These data were then evaluated by Dunnett's multiple comparison test to determine whether the expression rates at 35 mmHg and 75 mmHg were significantly higher than control rates at 10 mmHg.

### 2.3. ELISA

Seven eyes were examined by ELISA in each condition. After pressure loading, the retinal samples were rapidly homogenized in PBS followed by centrifugation at 4°C for 15 min at 3,000g. The supernatants were used to measure the concentrations of TSPO, 5aRD type I (5aRD1), 5aRD type II (5aRD2), and 5aRD type III (5aRD3) using corresponding ELISA kits (TSPO ELISA kit, Cat#CSB-EL025168RA, Cusabio, Wuhan, China; 5α-reductase I ELISA Kit, Cat#MBS700746-48TEST, MyBioSourc Inc., San Diego, CA; 5α-reductase II ELISA Kit, Cat#SEM285RA, Uscn Life Science, Houston, TX; 5α-reductase III ELISA Kit, Cat#MBS9320507, MyBioSourc Inc.). According to the manufacturer's instructions, the absorbance was detected at 450 nm and a standard curve was delineated based on the absorbance of standards. Each measurement of protein was normalized to 10 mmHg. These data were evaluated by Dunnett's multiple comparison test to determine whether the expression rates at 35 mmHg and 75 mmHg were significantly higher than control rates at 10 mmHg.

### 2.4. Immunohistochemistry

For immunocytochemistry, eyecup preparations were fixed with 4% paraformaldehyde-0.1 M phosphate buffer for 2 hours at 4°C (5 animals per experimental group) at the end of each experiment. Samples were washed with ice cold phosphate buffered saline (PBS) and incubated in blocking solution (1% donkey serum/PBS) for 2 h at 25°C. Samples were then embedded in OCT compound (Sakura Global Holdings, Tokyo, Japan), and frozen with liquid nitrogen. Ten μm cryosections were incubated with a primary antibody (Gavish et al.

1999, Papadopoulos et al., 2006) raised in sheep against 5α-reduced neurosteroids diluted 1:2500 in blocking solution for 24 h at 4°C. This polyclonal antibody primarily recognizes AlloP and has minimal cross-reactivity with other neurosteroids in rats (Veenman et al., 2007) (purchased from Dr. Robert Purdy, University of California San Diego). After incubation with primary antibody, slices were rinsed with PBS and incubated with a secondary antibody, biotinylated rabbit anti-sheep IgG (diluted 1:500) (Cat#BA-6000, AB_2336217, Vector Laboratories, Burlingame, CA). Other cryosections were incubated with rabbit anti-TSPO polyclonal antibody (1:50; Cat# LS-B2120-50, LifeSpan Biosciences, Inc., Seattle, WA), rabbit anti-5aRD1 polyclonal antibody (1:200; Cat#bs-11308R, Bioss Antibodies, Woburn, MA), rabbit anti-5aRD2 polyclonal antibody (1:200; Cat#bs-6700R, AB_11051640, Bioss Antibodies, Woburn, MA), or rabbit anti-5aRD type III (5aRD3) polyclonal antibody (1:200; Cat#GTX45982,GeneTex, Irvine, CA) at 4°C, overnight. Biotin-conjugated goat anti-rabbit IgG (H+L) (1:500; Zymed Laboratories, Carlsbad, CA) was applied to the sections incubated with primary antibody as a secondary antibody. After incubation with secondary antibodies, the slices were incubated with streptavidin conjugated with Alexa Fluor 488 (diluted 1:1000) (Cat#S32354, AB_2315383, Molecular Probes, Carlsbad, CA), for 2 h at 25°C. IgG binding sites were detected by confocal laser scanning microscopy (LSM510 Axiovert200M; Carl Zeiss Meditec, Göttingen, Germany). DAPI was used for nuclear staining.

For double immunofluorescence, cryosections of the fixed specimens were incubated at room temperature with a mixture of two primary antibodies: mouse anti-rat Thy 1.1 monoclonal antibody (1:100; Cat#551401, BD Bioscience, San Jose, CA) and rabbit anti-human GFAP antibody (1:200; Cat#SML-RO1003, Shima Laboratories Co., Tokyo, Japan). Subsequent antibody detection was performed with a mixture of two secondary antibodies, rhodamine-conjugated goat anti-mouse IgG (1:200) and FITC-conjugated goat anti-rabbit IgG (1:200; Cat#ab6717, Zymed Laboratories, Carlsbad, CA). After several washes with PBS, colocalization of vimentin was observed under a confocal microscope.

For quantification of immunohistochemical data, five eyes were examined in each condition. Images of each section without DAPI staining were captured. Digital images were analyzed, and the average intensity of FITC fluorescence was measured using Image-Pro Plus software (Media Cybernetics, Rockville, MD). All data of FITC fluorescence are expressed as mean ± SEM, and evaluated by Tukey's or Dunnett's multiple comparison test, or Mann-Whitney's U test compared to controls incubated in aCSF at 10 mmHg or 75 mmHg.

### 2.5. LC-MS/MS

For sample preparation, a rat retina was detached from the retinal pigment epithelium, and homogenized in 1 mL of 0.1 M potassium dihydrogen phosphate solution using an Ultra-Turrax homogenizer. Three eyes were examined by LC-MS/MS in each condition. As an internal standard, $^{2}H_{4}$-allopregnanolone was added to the rat retina suspension. AlloP was extracted by 4 mL of methyl *tert*-butyl ether (MTBE) from the remaining rat retina suspension. After the organic layer was evaporated to dryness, the extract was dissolved in 0.5 mL of methanol and diluted with 1 ml of distilled water, and then applied to adande:I PAX cartridge, which had been successively conditioned with 3 ml of methanol and 3 ml of

distilled water. After the cartridge was washed with 1 mL of distilled water, 1 mL of methanol/distilled water/acetic acid (45:55:1,v/v/v), and 1 mL of 1% pyridine solution, AlloP was eluted with 1 mL of methanol/pyridine (100:1,v/v). After evaporation, the residue was subjected to derivatization described below.

The sample was reacted with 50 μL of mixed solution (80 mg of 2-methyl-6-nitrobenzoic anhydride, 20 mg of 4-dimethylaminopyridine, and 40 mg of picolinic acid in 1 ml of acetonitrile) and 10 μl of triethylamine for 30 min at room temperature. After the reaction, the sample was dissolved in 0.5 ml of ethyl acetate/hexane/acetic acid (15:35:1, v/v) and the mixture was applied to InertSep SI cartridge, which had been successively conditioned with 3 mL of acetone and 3 mL of hexane. The cartridge was washed with 1 mL of hexane, 2 ml of ethyl acetate/hexane (3:7, v/v), and 2.5 mL of MTBE and then the derivatized AlloP was eluted with 2.5 mL of acetone/hexane (7:3, v/v). After evaporation, the residue was dissolved in 0.1 mL of acetonitrile/distilled water (2:3, v/v) and 20 μL of the solution was subjected to LC-MS/MS (Pesaresi et al., 2010).

An API-5000 triple stage quadrupole mass spectrometer (ABSCIEX) equipped with a positive ESI source and a HPLC system (SCL-10Avp system controller, LC-20AD pump, SIL-HTc column oven, CTO-20A auto-sampler, SHIMADZU) was employed. Capcellcore ADME column was used at 50°C. The mobile phase consisting of 0.1% formic aid (Solvent A) and acetonitrile/methanol (9:1, v/v) (Solvent B) was used with a gradient elution. For quantification of the steroids, the transitions *m/z* 424.4→283.3 and 428.4→287.3, were selected for AlloP and $^{2}H_{4}$-AlloP, respectively.

Changes in AlloP concentrations were evaluated by Tukey's multiple comparison test compared to controls incubated in aCSF at 10 mmHg or 75 mmHg.

### 2.6. Light Microscopy

At the end of each experiment, eyecup preparations were fixed in 2.5% glutaraldehyde in 0.1 M phosphate buffer overnight at 4°C. The fixed retinas were rinsed in 0.1 M phosphate buffer and placed in 1% buffered osmium tetroxide for 60 minutes. The retinas were dehydrated with an ethanol dilution series, embedded in epoxy resin (Epon 812, TAAB Laboratories, Aldermaston, UK) and cut into 1 μm thick semi-thin sections. The tissue was then stained with toluidine blue and evaluated by light microscopy.

### 2.7. Data analysis of morphometry

We examined the middle portion of the retina, greater than 1,200 μm away from the center of the optic disc along the inner limiting membrane (ILM) according to previously described methods (Ishikawa et al., 2011). The nerve fiber layer thickness (NFLT) was measured by light microscopy along 5 lines perpendicular to the pigment epithelium at a distance of 15 μm from each other around 1,200 μm away from the center of the optic disc (see Figure supplement S1). The average NFLT was determined in 5 different light micrographs taken from 3 to 5 eyecup samples in each condition, divided by total retinal thickness, and mean ± standard deviation was analyzed and compared with control.

The density of degenerated cells characterized by nuclear chromatin clumping or necrosis in the GCL was determined by counting 30 fields of 500 μm length at 10 different locations in light micrographs taken from the block of the middle retinal part 950 to 1450 μm away from the center of the optic disc (Ishikawa et al., 2014).

The severity of neuronal damage was assessed by light microscopy using a neuronal damage score (NDS) as previously described (Izumi et al., 1999). The NDS was determined in 5 different light micrographs taken from 3 to 5 eyecup samples in each condition. The NDS rates neuronal damage in the inner nuclear layer (INL) and the inner plexiform layer (IPL) on a 0–4 scale with 0 signifying no neuronal damage and 4 indicating very severe damage. Criteria used in establishing the degree of neuronal damage included the extent of cytoplasmic swelling in the IPL and the number of neurons in the INL showing signs of severe cytoplasmic swelling and coarse clumping of nuclear chromatin. The highest NDS rating (4) is given when the IPL shows apparent spongiform appearance due to dendritic swelling and when most cell bodies in the INL show severe cytoplasmic swelling and coarse clumping of nuclear chromatin. If the damage is of a lesser degree, a rating of 3 is given. NDS 2 is assigned when cell bodies in the INL are sporadically swollen. In NDS 1, damage does not fulfill higher criteria but the retinas differ from controls (NDS 0). Fine dendritic swelling in a limited area of the IPL without damage in the INL is described by NDS 1.

These morphometrical parameters were assessed by three raters, who remained unaware of the experimental condition. Upon completion of data assessment, significance of individual differences among raters was evaluated using five randomly selected samples in each morphometric parameter by one-way analysis of variance (one-way ANOVA) followed by a post-hoc test. There were no significant differences among the raters in any of the morphometric measurements. All data of the NFLT, NDS, and the density of degenerated cells in the GCL are expressed as mean ± SEM, and evaluated by Dunnett's multiple comparison test compared to controls incubated in aCSF at 10 mmHg or 75 mmHg.

### 2.8. Electron Microscopy

Retinal specimens were trimmed to a smaller size, and ultrathin sections (75 nm) were cut with a diamond knife and suspended over formvar-coated slot grids (1 # 2 mm opening). The sections were stained with uranyl acetate and lead citrate and viewed in a transmission electron microscope (H-7650, Hitachi High-Technologies Corp., Tokyo, Japan).

### 2.9. Preparation of whole mounted retinas and immunostaining

The anterior part of the eye was removed by making an incision along the entire limbus. After incubation in the closed pressure system, retinas from five eyes in each group were processed for immunostaining as "whole mounted" retinas. The retina was carefully detached from the eye by making cuts along the ora serrata and optic nerve. Whole retinas were then flat-mounted, pinned in an acrylic plate with the RGC layer facing upward using stainless steel pins, and fixed in 4% paraformaldehyde-0.1 M phosphate buffer overnight at 4°C. After the samples were fixed, the tissue was rinsed with PBS three times. To block nonspecific binding, the tissue was incubated in 2% BSA in PBS containing 0.5% Triton X-100. The whole mounted retinas were incubated in the rabbit anti-NeuN polyclonal

antibody solution (Cat#ab104225, Abcam) (1:100) by gently shaking at 4 °C, overnight. After rinsing 3 times using PBS, the retina was incubated in FITC-conjugated secondary antibody (goat anti-rabbit IgG (H+L)) (Cat#81-6111, Zymed Laboratories Inc) (1:300). The retina tissue was then rinsed 3 times with PBS and mounted on glass slides using 50% PBS and 50% glycerol. Retinal flat-mounts were imaged throughout the GCL in each of the four defined retinal quadrants 4 mm from the optic nerve head using a confocal microscope. Each quadrant was analyzed using a 1 $mm^2$ frame, and counted using Image-Pro Plus software. The density of NeuN positive RGCs per square millimeter was averaged and compared in experimental retinas treated with 1 μM AlloP or 50 μM PK11195 at 75 mmHg and control retinas incubated with aCSF at 75 mmHg by Dunnett's multiple comparison test. RGC counts were analyzed using Image-Pro Plus software.

### 2.10. Apoptosis

To visualize apoptotic cells, we used the DeadEndTM Colorimetric TUNEL System (Promega, Madison, WI) according to the manufacturer's instructions. The nuclei were counterstained with DAPI. After the length of each retinal section was measured (Image-Pro Plus software), the cells were counted in the whole section length and the number of cells was counted per 200 μm of retinal section.

The number of apoptotic cells was evaluated by Dunnett's multiple comparison test to determine changes in the density of apoptotic cells among experimental retinas treated with 1 μM AlloP or 50 μM PK11195 at 75 mmHg and control retinas incubated with aCSF at 75 mmHg.

### 2.11. Chemicals

Atriol (Midzak et al., 2011) was synthesized by D.F.C. MK801 (Cat#F1293-100MG, CAS.NO 98319-26-7) and PK11195 (Cat#C0424-50MG, CAS.NO 85532-75-8)[38] were purchased from Sigma-Aldrich Corp (St. Louis, MO, USA). AlloP was purchased from Wako Pure Chemical Industries, Ltd. (Cat#596-30841, CAS.NO 516-54-1; Osaka, Japan). Dutasteride was obtained from Adooq Bioscience LLC (Cat#A10338, CAS.NO 164656-23-9, Irvine, CA, USA). All other chemicals were purchased from Sigma-Aldrich Corp. or Nacalai Tesque (Kyoto, Japan). Atriol, MK-801, AlloP, PK11195, and dutasteride were dissolved in dimethyl sulfoxide (DMSO) as a 10 mM stock solution.

### 2.12. Statistics

Data were double-checked and analyzed using a biomedical statistical computer program (http://www.gen-info.osaka-u.ac.jp/MEPHAS/dunnett.html) on a personal computer. Descriptive statistical results were presented using the mean values (mean) ± standard deviation (SD). For comparison with controls that were incubated in drug free aCSF at 10 mmHg, we used Mann-Whitney's U test or Dunnett's multiple comparison test, depending on sample numbers. For comparison with both the control and other conditions, we used Tukey's multiple comparison test. For all analyses, p values were considered statistically significant, when the values were less than 0.05 (two-tailed).

## 3. Results

### 3.1. Pressure elevation induced upregulation of TSPO

Using quantitative real-time RT–PCR, we determined that *tspo* expression increased in a pressure-dependent manner (Fig. 1c, Source data S1-1). *Tspo* mRNA showed significant increases at 35 mmHg ($p<0.05$) and 75 mmHg ($p<0.05$) compared to 10 mmHg. Consistent with this, the ELISA test for TSPO protein expression also detected significant increases at 35 mmHg ($p<0.05$) and 75 mmHg ($p<0.05$) compared to 10 mmHg (Fig. 1d, Source data S1-2). We also tested if TSPO immunostaining was altered by elevated pressure. TSPO immunostaining was negligible or slight at 10 mmHg (Fig. 1e) and weakly positive in the vicinity of the ganglion cell layer (GCL) at 35 mmHg, respectively (Fig. 1f). TSPO expression increased in the RGC at 75 mmHg (Fig. 1g, Figure supplement S2). Fluorescence intensities in each condition are summarized in Fig. 1h (Source data S1-3).

### 3.2. Pressure elevation induced upregulation of 5aRD subclasses

Because elevated pressure enhances AlloP synthesis (Ishikawa et al., 2014), we hypothesized that 5aRD expression would be facilitated by elevated pressure. Using quantitative real-time RT–PCR, we examined the effect of pressure on *srd5a* subclasses (Fig. 2a, Source data S2-1). Expression of *srd5a1* mRNA showed no remarkable changes at 35 mmHg, but significantly increased at 75 mmHg ($p<0.05$) compared to 10 mmHg (Source data S2-1-1). *Srd5a2* mRNA showed a significant increase at 35 mmHg ($p<0.05$) and 75 mmHg ($p<0.05$) compared to 10 mmHg (Source data S2-1-2). *Srd5a3* mRNA expression showed no remarkable change at elevated pressures (Source data S2-1-3).

We also examined pressure-dependent changes of protein expression of 5aRD1, 5aRD2, and 5aRD3 using ELISA (Fig. 2b) and immunohistochemistry (Fig. 2c–2k). The ELISA test showed that there was no remarkable change in 5aRD1 expression at 35 mmHg, but 5aRD1 expression significantly increased at 75 mmHg ($p<0.05$) compared to 10 mmHg (Source data S2-2-1). 5aRD2 expression significantly increased at 35 mmHg ($p<0.05$) and 75 mmHg ($p<0.05$) compared to 10 mmHg (Source data S2-2-2). 5aRD3 expression showed no significant increase at 35 mmHg and 75 mmHg compared to 10 mmHg (Source data S2-2-3).

In immunohistochemistry studies, 5aRD1 reactivity was slight at 10 mmHg (Fig. 2c) and 35 mmHg (Fig. 2d), but significantly increased at 75 mmHg, mainly in the GCL and INL (Fig. 2e). 5aRD2 immunostaining was marginal at 10 mmHg (Fig. 2f). Only slight immunofluorescence was detected in the vicinity of the GCL and INL at 35 mmHg (Fig. 2g), while a marked increase of immunofluorescence was observed in the GCL and INL at 75 mmHg (Fig. 2h). 5aRD3 immunostaining was negligible at all pressures (Fig. 2i–k). Fluorescence intensities in each condition are summarized in Figure 2l (Source data S2-3). 5aRD1 immunostaining showed a significant increase at 75 mmHg ($p<0.05$) compared to 10 mmHg. 5aRD2 immunostaining significantly increased at 35 mmHg ($p<0.05$) and 75 mmHg ($p<0.05$) compared to 10 mmHg.

### 3.3. Pressure elevation induced neurosteroidogenesis

We confirmed our prior observations about the effects of elevated hydrostatic pressure on neurosteroid immunostaining using an antibody against 5α-reduced steroids that primarily recognizes AlloP (anti-AlloP antibody) (Ishikawa et al., 2014). Immunostaining was negligible at 10 mmHg (Fig. 3a). A slight fluorescent reaction was observed in the GCL at 35 mmHg (Fig. 3b), while at 75 mmHg, positive AlloP immunofluorescence was clearly detected in the GCL and INL (Fig. 3c). Fluorescence intensities at each pressure are summarized in Figure 3d (Source data S3-1). Quantitative analysis confirmed that AlloP immunostaining significantly increased at 75 mmHg ($p<0.05$) compared to 10 mmHg.

### 3.4. Changes of neurosteroidogenesis by TSPO ligands and 5aRD inhibitor

In immunohistochemistry studies, the enhanced staining with anti-AlloP antibody induced by elevated hydrostatic pressure was significantly dampened by incubation with 1 μM atriol (Fig. 3e). This result indicates that TSPO is essential for AlloP production by elevated pressure (Yang 2004). Anti-AlloP immunostaining was also eliminated in retinas treated with 1 μM dutasteride, a 5aRD inhibitor, at 75 mmHg (Fig. 3f). PK11195, a TSPO ligand, increased immunofluorescence by anti-AlloP antibody in the GCL, IPL, INL, ONL, and OLM at 75 mmHg (Fig. 3g). This enhancement of AlloP fluorescence was inhibited by 1 μM atriol (Fig. 3h) or 1 μM dutasteride (Fig. 3i). Fluorescence intensities at each condition are summarized in Figure 3j (Source data S3-2). Quantitative analysis confirmed that administration of atriol or dutasteride resulted in a significant decrease in AlloP immunostaining at 75 mmHg ($p<0.05$) compared to controls incubated with aCSF at 75 mmHg. The increase in AlloP immunoreaction induced by PK11195 was also dampened by atriol or dutasteride compared to controls incubated with aCSF at 75 mmHg.

At 10 mmHg, PK11195 enhanced AlloP labeling in the GCL, IPL, and INL (Fig. 4a). PK11195-mediated enhancement of AlloP fluorescence was inhibited by 1 μM atriol (Fig. 4b) or 1 μM dutasteride at 10 mmHg (Fig. 4c). Fluorescence intensities of AlloP in each condition are summarized in Figure 4d (Source data S4-1). Enhancement in AlloP immunoreaction induced by PK11195 was significantly inhibited by atriol or dutasteride. compared to controls incubated with aCSF at 10 mmHg.

Because PK11195 promoted AlloP synthesis, we hypothesized that PK11195 might also enhance the expression of TSPO and 5aRD at each pressure. With immunohistochemistry, we examined the fluorescence reaction of TSPO and 5aRD2 in retinas treated with 50 μM PK11195. PK11195 markedly enhanced TSPO labeling in the GCL, IPL, INL, OPL, ONL, and OLM compared to controls incubated without PK11195 at 75 mmHg (Fig. 4e, 4f, Source data S4-2). PK11195 also increased immunofluorescence by anti-TSPO antibody in the GCL, IPL, INL, and OPL compared to controls incubated without PK11195 even at 10 mmHg (Fig. 4g, 4h, Source data S4-3). At 75 mmHg, PK11195 enhanced immunofluorescence in the GCL, INL, and ONL against 5aRD2 compared to controls incubated without PK11195 (Fig. 4i, 4j, Source data S4-4). PK11195 also increased 5aRD2-immunofluorescence in the GCL and INL compared to controls incubated without PK11195 even at 10 mmHg (Fig. 4k, 4l, Source data S4-5).

### 3.5. LC-MS/MS

LC-MS/MS analysis revealed significant increases in AlloP levels at 75 mmHg ($p<0.05$) but not at 35 mmHg compared to 10 mmHg (Fig. 5a, Source data S5-1).

Consistent with the results in immunohistochemistry, the increase in AlloP synthesis induced by high pressure was significantly diminished by 1 μM atriol, a TSPO antagonist (Midzak et al., 2011) or 1 μM dutasteride, a 5aRD inhibitor ($p<0.05$), indicating that the increase in AlloP synthesis by elevated pressure is mediated by TSPO and 5aRD. Administration of 50 μM PK11195, a TSPO ligand, significantly increased AlloP synthesis at 75 mmHg ($p<0.05$) compared to retinas incubated without PK11195 at 75 mmHg. Enhancement of AlloP production by PK11195 was inhibited by 1 μM atriol and 1 μM dutasteride at 75 mmHg ($p<0.05$) compared to retinas incubated without PK11195 at 75 mmHg (Fig. 5b, Source data S5-2).

LC-MS/MS analysis also revealed that administration of 50 μM PK11195 significantly increased AlloP synthesis even at 10 mmHg ($p<0.05$) compared to retinas incubated without PK11195 at 10 mmHg. Enhancement of AlloP production by PK11195 was inhibited by 1 μM atriol and 1 μM dutasteride at 10 mmHg ($p<0.05$) compared to retinas incubated without PK11195 at 10 mmHg (Fig. 5c, Source data S5-3).

### 3.6. Effects of pressure elevation on retinal morphology

We also examined the effects of pressure elevation on retinal morphology. Consistent with our previous reports (Ishikawa et al., 2010, 2011, 2014), retinas incubated at 10 mmHg (Fig. 6a) or 35 mmHg (Fig. 6b) exhibited a normal appearance. Retinas incubated at 75 mmHg showed axonal swelling in the NFL as previously reported (Fig. 6c, 6d) (Ishikawa et al., 2014). Immunohistochemical double staining revealed that the swollen axons of the RGC were specifically labeled with anti-Thy 1.1 antibody, an axonal marker of RGCs (Mata et al., 2015) (Fig. 6e). We found no colocalization of anti-Thy 1.1 antibody with anti-GFAP antibody, a glia marker whose expression is augmented in Müller cells following high pressure incubation (Ishikawa et al., 2010) (Fig. 6e). Electron microscopy revealed substantial axonal swelling in the NFL after exposure to high pressure (75 mmHg; Fig. 6f–6h) compared with control retinas incubated at 10 mm Hg (Fig. 6i). Elevated pressure also increased the number of degenerated cells (Fig. 6j) or apoptotic cells with chromatin condensation at the edge of the nucleus (Fig. 6k).

A quantitative assessment of structural changes induced by pressure elevation is summarized in Table 2 (Source data S6). The NFLT in retinas incubated at 75 mmHg was significantly increased compared to control retinas incubated at 10 mm Hg ($p<0.05$). NDS were also significantly increased after exposure to high pressure (75 mmHg) ($p<0.05$). At 75 mmHg, the density of damaged cells in the GCL was greater in retinas incubated at 75 mmHg compared to control retinas incubated at 10 mmHg.

### 3.7. Effects of pressure and TSPO ligands on retinal morphology

Consistent with our previous study (Ishikawa et al., 2014), we found that exogenously administered AlloP attenuated the development of axonal swelling at high pressure (Figure

supplement S3a). This prompted us to test whether atriol or dutasteride, which block endogenous AlloP production, worsens the histological changes induced by elevated pressure. Retinas incubated in 1 μM atriol with high pressure exhibited severe damage characterized by edematous changes in the IPL and bull's eye cellular formation in the INL, characterized by nuclear pyknosis with pale cytoplasm, along with axonal swelling (Fig. 7a). The damage by atriol at 75 mmHg was substantially diminished by 1 μM AlloP (Figure supplement S3b) and also by 1 μM MK801 (Figure supplement S3c), indicating that TSPO activation resulting in AlloP synthesis helps to prevent NMDA receptor-mediated damage at high pressure. Dutasteride (1 μM) also induced excitotoxic changes characterized by bull's eye formation in the INL and edematous changes in the IPL along with axonal swelling in the NFL (arrowheads) at 75 mmHg (Fig. 7b).

We then examined the effects of the PK11195, which enhances AlloP production, on retinal morphology. At 75 mmHg administration of PK11195 substantially inhibited axonal swelling without showing excitotoxic retinal damage (Fig. 7c). In the presence of PK11195, 1 μM atriol induced severe neuronal damage and axonal swelling at 75 mmHg (Fig. 7d). Because the enzymatic reaction by 5aRD occurs downstream of the translocation of cholesterol to the inner mitochondrial membrane by TSPO (Rupprecht et al., 2010), we also examined the effects of the 5aRD inhibitor, dutasteride, against the neuroprotective effects of PK11195. At 75 mmHg, dutasteride induced severe neuronal damage in addition to axonal swelling in spite of the presence of PK11195 (Fig. 7e). These results indicate that enhanced AlloP production via sequential activation of TSPO and 5aRD is necessary for PK11195-mediated neuroprotection. Exogenous 1 μM AlloP restored protection in the presence of atriol and PK11195 (Figure supplement S3d).

Electron microscopy revealed that the combination of high pressure and atriol (1 μM) resulted in degeneration of swollen axons (Fig. 7f). Dutasteride (1 μM) also induced degeneration of swollen axons (Fig. 7g) and marked accumulation of degenerated cell organelles or electron-dense materials in the swollen axons (Fig. 7h). The combination of high pressure and PK11195 also induced marked axonal swelling in the presence of atriol (Fig. 7i) or dutasteride (Fig. 7j).

A quantitative assessment of structural changes induced by pressure elevation and/or administration of atriol, dutasteride, or PK11195 is summarized in Table 3 (Source data S7). The increase in the NFLT, NDS, and the density of the damaged cells in the GCL induced by exposure to 75 mmHg was significantly decreased by PK11195 at 75 mmHg compared to controls incubated in aCSF at 75 mmHg ($p<0.05$). The NDS and the density of the damaged cells in the GCL were significantly increased by administration of 1 μM atriol, 1 μM dutasteride, a combination of PK11195 and atriol, or PK11195 and dutasteride compared to control incubated in aCSF at 75 mmHg ($p<0.05$).

### 3.8. Effects of pressure elevation on RGCs and neuroprotection with AlloP and PK11195 in whole mounted retinas

In whole mounted retinas, RGC damage induced by pressure elevation was visualized as reduced numbers of cells that were positive for NeuN (Figure 8a, b). Fig. 8a illustrates examples of confocal images of NeuN-labeled RGCs that were obtained from a control eye

incubated at 10 mmHg. Pressure elevation (75 mmHg) reduced the number of cells that were positive for NeuN (Fig. 8b). The confocal images in Fig. 8c and Fig. 8d illustrate the neuroprotective effects of AlloP (1 μM) and PK11195 (50 μM) on RGC survival in hyperbaric conditions, respectively. The graph in Fig. 8e shows the number of NeuN-positive RGCs in the retina in each condition (Source data S8-1).

### 3.9. Pressure-induced apoptosis and neuroprotection with AlloP and PK11195

At 10 mmHg, a few TUNEL-positive cells are observed only in the GCL and ONL (Fig. 8f). Exposure to elevated pressure induced apoptosis that was apparent in the GCL and to a lesser extent in the INL (Fig. 8g). The number of TUNEL-positive cells was reduced when 1 μM AlloP (Fig. 8h) or 50 μM PK11195 (Fig. 8i) was administered. The graph in Fig. 8j shows the number of apoptotic cells in the retina in each condition (Source data S8-2).

## 4. Discussion

In the present study, we used an *ex vivo* model that incubated dissected rat eyecups under pressure for 24 hours in a newly developed closed pressure-loading system. The pressure was adjusted to simulate conditions in the normal retina (10 mmHg) and conditions that can occur during an acute angle closure attack (75 mmHg). This model avoids the influence of circulating steroids, making it possible to investigate direct effects of pressure-loading on neurosteroidogenesis. In the process of endogenous AlloP synthesis, translocation of cholesterol to the inner mitochondrial membrane by TSPO (Rupprecht et al., 2010) and the catalytic reaction by 5aRD (Dong et al., 2001; Agis-Balboa et al., 2007) are considered rate limiting steps. In the present study, quantitative real-time PCR, ELISA, and immunohistochemistry demonstrated that pressure loading induced upregulation of both TSPO and subclasses of 5aRD (mainly type 2).

TSPO, previously called the peripheral benzodiazepine receptor, is localized predominantly on the outer mitochondrial membrane (Culty et al., 1999). In the central nervous system, TSPO is expressed in both glial cells and neurons (Tokuda et al., 2010; Veiga et al., 2005), and is reported to participate in a variety of processes including apoptosis, glial proliferation (Casellas et al., 2002; Gavish et al., 1999; Papadopoulos et al., 2006; Veenman et al., 2007), and cellular pathology (Veiga et al., 2005; Vowinckel et al., 1997; Yasuno et al., 2008; Rupprecht et al., 2010; Edison et al., 2008; Meßmer and Reynolds, 1998; Cosenza-Nashat et al., 2009; Gerhard et al., 2005; Turner et al., 2004; Ouchi et al., 2005). In the retina, TSPO is significantly upregulated in microglia in mouse models of retinal inflammation and injury (Wang et al., 2014; Karlstetter et al., 2014). However, changes in TSPO expression have not been examined in glaucoma models. The present immunostaining studies demonstrate that expression of TSPO is markedly enhanced in the inner retina including RGC under hyperbaric conditions. Because the present study indicates that TSPO is colocalized with 5aRD and AlloP in RGC, it appears that RGC are the principal site of retinal neurosteroid synthesis under hyperbaric conditions.

Our previous study (Ishikawa et al., 2014) demonstrated that dutasteride, an inhibitor of both 5aRD1 and 5aRD2 (Tian, 1994), dampened AlloP synthesis more effectively than finasteride, an agent that primarily inhibits 5aRD2 with less effect on 5aRD1 (Nickel, 2004).

Based on these results, it is likely that both 5aRD1 and 5aRD2 contribute to AlloP production in the pressure-loaded retina. Consistent with these findings, we observed significant increases in 5aRD2 expression and less preferential increases in 5aRD1 at 75 mmHg in three different sets of experiments in the present study. The present quantitative real-time RT-PCR, ELISA, and immunostaining studies reveal no remarkable changes in 5aRD3 expression, indicating that 5aRD3 is unlikely to play a major role in neurosteroidogenesis under pressure-loading.

Finasteride is approved by the Food and Drug Administration for treatment of benign prostatic hyperplasia (BPH) and androgenic alopecia, while dutasteride is used for treatment of BPH. Thus, it is plausible that significant numbers of men with glaucoma take 5aRD inhibitors. Visual impairment has been reported with finasteride in a glaucoma patient (Lee and Lee, 2013), raising the possibility that glaucoma patients taking 5aRD inhibitors may be at risk of retinal damage as a result of inhibition of AlloP synthesis during periods of elevated IOP. Because administration of finasteride also induces excitotoxic neuronal cell death in the hippocampus and cerebellum in fetal sheep brain (Yawno et al., 2009), risk may extend to other brain regions.

In the present study, we determined whether AlloP synthesis requires TSPO. As our results show, the increase in AlloP synthesis induced by high pressure is significantly diminished by 1 μM atriol, an agent that preferentially inhibits TSPO (Midzak et al., 2011). This finding strongly suggests that the increase in AlloP synthesis by high pressure requires TSPO, and is mediated, at least in part, by induction of TSPO expression. Additionally, we found that administration of atriol in the presence of high pressure resulted in retinal degeneration with edematous changes in the IPL and bull's eye cellular formation in the INL, findings that are characteristic of excitotoxic retinal damage (Izumi et al., 1995; Izumi et al., 1999). To determine the contribution of excitotoxicity to this retinal degeneration, we examined MK801, a NMDA receptor antagonist, in atriol-treated retinas under hyperbaric conditions, and found that MK801 substantially inhibited atriol-associated retinal degeneration. These findings indicate that atriol promotes excitotoxicity in pressure-loaded retinas by inhibiting neurosteroidogenesis. Protection against atriol-induced excitotoxicity by exogenously administered AlloP further suggests the therapeutic potential of AlloP and related compounds.

It has long been thought that PK11195, which binds the peripheral benzodiazepine receptor, acts as a TSPO antagonist. However, other studies reveal that PK11195 has at least partial agonist activity at TSPO, depending upon cell type and drug concentration (Shany et al., 1994; Choi et al., 2010). Indeed, in our rat *ex vivo* glaucoma model, PK11195 clearly enhanced actions mediated by TSPO, indicating that PK11195, at the concentration used in the current study, behaves as a TSPO agonist at both 10 mmHg and 75 mmHg, and prevents pressure-induced RGC injury and apoptotic RGC death. Consistently, atriol and dutasteride, both of which block AlloP synthesis by inhibition of TSPO and 5aRD, respectively, reversed the neuroprotective effects of PK11195, indicating that PK11195 exerts its neuroprotection by AlloP synthesis via sequential activation of TSPO and 5aRD. These results indicate that PK11195 or other TSPO agonists may be useful in protecting glaucomatous eyes from pressure-induced excitotoxic degeneration by induction of AlloP synthesis.

Preliminary studies in humans indicate that TSPO agonists have anxiolytic effects mediated by AlloP (Rupprecht et al., 2009). A potential problem in the use of TSPO agonists is that these agents would likely increase AlloP concentration in the systemic circulation, possibly resulting in negative feedback effects against local neurosteroidogenesis. Another significant concern is that neurosteroids are very potent and effective modulators of tonic and phasic GABAergic inhibition, resulting in sedation, incoordination, cognitive impairment and other side effects that could limit therapeutic use. In both rodents and humans, however, studies to date indicate that TSPO agonists do not appear to cause significant adverse effects (Rupprecht et al., 2009; Marx et al., 2011; Zorumski et al., 2013).

Taken together, our findings indicate that enhanced AlloP synthesis mediated by TSPO and 5aRD has important roles in maintaining retinal integrity under hyperbaric conditions. TSPO agonists and GABAergic neuroactive steroids have potential as therapeutic agents to protect glaucomatous eyes from pressure-induced injuries.

## Supplementary Material

Refer to Web version on PubMed Central for supplementary material.

## Acknowledgments

**Grant information:** This work was supported in part by JST Grant no. AS242Z03426Q to M.I., JSPS KAKENHI Grant No. 24592666 to M.I., JSPS KAKENHI Grant No. 25462750 to T.Y., and National Institute of Health grants MH077791 and MH101874, and the Bantly Foundation to C.F.Z.

The authors thank Sanae Takaseki for technical support and Kathiresan Krishnan for synthesizing the atriol in the laboratory of D.F.C.

## References

Agis-Balboa RC, Pinna G, Pibiri F, Kadriu B, Costa E, Guidotti A. Downregulation of neurosteroid biosynthesis in corticolimbic circuits mediates social isolation-induced behavior in mice. Proc Natl Acad Sci USA. 2007; 104:18736–18741. [PubMed: 18003893]

Aung T, Ang LP, Chan SP, Chew PT. Acute primary angle-closure: long-term intraocular pressure outcome in Asian eyes. Am J Ophthalmol. 2001; 131:7–12. [PubMed: 11162972]

Bailey JN, Yaspan BL, Pasquale LR, Hauser MA, Kang JH, Loomis SJ, Brilliant M, Budenz DL, Christen WG, Fingert J, Gaasterland D, Gaasterland T, Kraft P, Lee RK, Lichter PR, Liu Y, McCarty CA, Moroi SE, Richards JE, Realini T, Schuman JS, Scott WK, Singh K, Sit AJ, Vollrath D, Wollstein G, Zack DJ, Zhang K, Pericak-Vance MA, Allingham RR, Weinreb RN, Haines JL, Wiggs JL. Hypothesis-independent pathway analysis implicates GABA and acetyl-CoA metabolism in primary open-angle glaucoma and normal-pressure glaucoma. Hum Genet. 2014; 133:1319–1330. [PubMed: 25037249]

Belelli D, Lambert JJ. Neurosteroids: endogenous regulators of the $GABA_A$ receptor. Nat Rev Neurosci. 2005; 6:565–575. [PubMed: 15959466]

Casellas P, Galiegue S, Basile AS. Peripheral benzodiazepine receptors and mitochondrial function. Neurochem Int. 2002; 40:475–486. [PubMed: 11850104]

Choi J, Ifuku M, Noda M, Guilarte TR. Translocator protein (18 kDa) peripheral benzodiazepine receptor specific ligands induce microglia functions consistent with an activated state. Glia. 2010; 59:219–230.

Cosenza-Nashat M, Zhao ML, Suh HS, Morgan J, Natividad R, Morgello S, Lee SC. Expression of the translocator protein of 18 kDa by microglia, macrophages and astrocytes based on

immunohistochemical localization in abnormal human brain. Neuropathol Appl Neurobiol. 2009; 35:306–328. [PubMed: 19077109]

Culty M, Li H, Boujrad N, Amri H, Vidic B, Bernassau JM, Reversat JL, Papadopoulos V. In vitro studies on the role of the peripheral type benzodiazepine receptor in steroidogenesis. J Steroid Biochem Mol Biol. 1999; 69:123–130. [PubMed: 10418986]

Diekmann H, Fischer D. Glaucoma and optic nerve repair. Cell Tissue Res. 2013; 353:327–337. [PubMed: 23512141]

Dong E, Matsumoto K, Uzunova V, Sugaya I, Takahata H, Nomura H, Watanabe H, Costa E, Guidotti A. Brain 5alpha-dihydroprogesterone and allopregnanolone synthesis in a mouse model of protracted social isolation. Proc Natl Acad Sci USA. 2001; 98:2849–2854. [PubMed: 11226329]

Gavish M, Bachman I, Shoukrun R, Katz Y, Veenman L, Weisinger G, Weizman A. Enigma of the peripheral benzodiazepine receptor. Pharmacol Rev. 1999; 51:629–650. [PubMed: 10581326]

Gerhard A, Schwarz J, Myers R, Wise R, Banati RB. Evolution of microglial activation in patients after ischemic stroke: a [11C](R)-PK11195 PET study. NeuroImage. 2005; 24:591–595. [PubMed: 15627603]

Gunn BG, Brown AR, Lambert JJ, Belelli D. Neurosteroids and $GABA_A$ receptor interactions: a focus on stress. Front Neurosci. 2011; 5:1–20. [PubMed: 21390287]

Harada T, Harada C, Nakamura K, Quah HM, Okumura A, Namekata K, Saeki T, Aihara M, Yoshida H, Mitani A, Tanaka K. The potential role of glutamate transporters in the pathogenesis of normal tension glaucoma. J Clin Invest. 2007; 117:1763–1770. [PubMed: 17607354]

Ishikawa M, Yoshitomi T, Zorumski CF, Izumi Y. Effects of acutely elevated hydrostatic pressure in the rat ex vivo retinal preparation. Invest Ophthalmol Vis Sci. 2010; 51:6414–6423. [PubMed: 20688725]

Ishikawa M, Yoshitomi T, Zorumski CF, Izumi Y. Downregulation of glutamine synthetase via GLAST suppression induces retinal axonal swelling in a rat ex vivo hydrostatic pressure model. Invest Ophthalmol Vis Sci. 2011; 52:6604– 6616. [PubMed: 21775659]

Ishikawa M, Yoshitomi T, Zorumski CF, Izumi Y. Neurosteroids are endogenous neuroprotectants in an ex vivo glaucoma model. Invest Ophthalmol Vis Sci. 2014; 155:8531–8541.

Izumi Y, Benz AM, Kurby CO, Labruyere J, Zorumski CF, Price MT, Olney JW. An ex vivo rat retinal preparation for excitotoxicity studies. J Neurosci Methods. 1995; 60:219–225. [PubMed: 8544482]

Izumi Y, Kirby CO, Benz AM, Olney JW, Zorumski CF. Müller cell swelling, glutamate uptake, and excitotoxic neurodegeneration in the isolated rat retina. Glia. 1999; 25:379–389. [PubMed: 10028920]

Kalloniatis M, Tomisich G. Amino acid neurochemistry of the vertebrate retina. Prog Retin Eye Res. 1999; 18:811–866. [PubMed: 10530752]

Karlstetter M, Nothdurfter C, Aslanidis A, Moeller K, Horn F, Scholz R, Neumann H, Weber BH, Rupprecht R, Langmann T. Translocator protein (18 kDa) (TSPO) is expressed in reactive retinal microglia and modulates microglial inflammation and phagocytosis. J Neuroinflam. 2014; 11:1–13.

Kishida K, Naka KI. Interaction of excitatory and depressant amino acids in the frog retina. J Neurochem. 1968; 15:833–841. [PubMed: 18561497]

Lee JW, Lee HJ. Reversible visual loss caused by combination therapy of alfuzosin and finasteride in a patient with uveitic glaucoma. Cutan Ocul Toxicol. 2013; 32:182–184. [PubMed: 23094797]

Louzada-Junior P, Dias JJ, Santos WF, Lachat JJ, Bradford HF, Coutinho-Netto J. Glutamate release in experimental ischaemia of the retina: an approach using microdialysis. J Neurochem. 1992; 59:358–363. [PubMed: 1351929]

Lowe RF. Primary angle-closure glaucoma: a review 5 years after bilateral surgery. Br J Ophthalmol. 1973; 57:457–463. [PubMed: 4725853]

Lucas DR, Newhouse JP. The toxic effect of sodium l-glutamate on the inner layers of the retina. Arch Ophthalmol. 1957; 58:193–201.

Martin KR, Levkovitch-Verbin H, Valenta D, Baumrind L, Pease ME, Quigley HA. Retinal glutamate transporter changes in experimental glaucoma and after optic nerve transection in the rat. Invest Ophthalmol Vis Sci. 2002; 43:2236–2243. [PubMed: 12091422]

Marx CE, Bradford DW, Hamer RM, Naylor JC, Allen TB, Lieberman JA, Strauss JL, Kilts JD. Pregnenolone as a novel therapeutic candidate in schizophrenia: emerging preclinical and clinical evidence. Neuroscience. 2011; 191:78–90. [PubMed: 21756978]

Massey SC, Miller RF. Excitatory amino acid receptors of rod- and cone-driven horizontal cells in the rabbit retina. J Neurophysiol. 1987; 57:645–659. [PubMed: 3031231]

Massey SC, Miller RF. N-Methyl-D-aspartate receptors of ganglion cells in rabbit retina. J Neurophysiol. 1990; 63:16–30. [PubMed: 2153770]

Mata D, Linn DM, Linn CL. Retinal ganglion cell neuroprotection induced by activation of alpha7 nicotinic acetylcholine receptors. Neuropharmacology. 2015; 99:337–346. [PubMed: 26239818]

Messmer K, Reynolds GP. Increased peripheral benzodiazepine binding sites in the brain of patients with Huntington's disease. Neurosci Lett. 1998; 241:53–56. [PubMed: 9502214]

Midzak A, Akula N, Lecanu L, Papadopoulos V. Novel androstenetriol interacts with the mitochondrial translocator protein and controls steroidogenesis. J Biol Chem. 2011; 286:9875–9887. [PubMed: 21209087]

Moreno MC, de Zavalía N, Sande P, Jaliffa CO, Fernandez DC, Keller Sarmiento MI, Rosenstein RE. Effect of ocular hypertension on retinal GABAergic activity. Neurochem Int. 2008; 52:675–682. [PubMed: 17928106]

Moreno MC, Sande P, Marcos HA, de Zavalía N, Keller Sarmiento MI, Rosenstein RE. Effect of glaucoma on the retinal glutamate/glutamine cycle activity. FASEB J. 2005; 19:1161–1162. [PubMed: 15870062]

Naskar R, Vorwerk CK, Dreyer EB. Concurrent downregulation of a glutamate transporter and receptor in glaucoma. Invest Ophthalmol Vis Sci. 2000; 41:1940–1944. [PubMed: 10845620]

Neal MJ, Cunningham JR, Hutson PH, Hogg J. Effects of ischaemia on neurotransmitter release from the isolated retina. J Neurochem. 1994; 62:1025–1033. [PubMed: 7906713]

Nickel JC. Comparison of clinical trials with finasteride and dutasteride. Rev Urol Suppl. 2004; 9:S31–S39.

Nucci C, Tartaglione R, Rombola L, Morrone LA, Fazzi E, Bagetta G. Neurochemical evidence to implicate elevated glutamate in the mechanisms of high intraocular pressure (IOP)-induced retinal ganglion cell death in rat. Neurotoxicology. 2005; 26:935–941. [PubMed: 16126273]

Olney JW. The toxic effects of glutamate and related compounds in the retina and the brain. Retina. 1982; 2:341–359. [PubMed: 6152914]

Ouchi Y, Yoshikawa E, Sekine Y, Futatsubashi M, Kanno T, Ogusu T, Torizuka T. Microglial activation and dopamine terminal loss in early Parkinson's disease. Ann Neurol. 2005; 57:168–175. [PubMed: 15668962]

Papadopoulos V, Lecanu L, Brown RC, Han Z, Yao ZX. Peripheral-type benzodiazepine receptor in neurosteroid biosynthesis, neuropathology and neurological disorders. Neuroscience. 2006; 138:749–756. [PubMed: 16338086]

Pascolini D, Mariotti SP. Global estimates of visual impairment. Br J Ophthalmol. 2012; 96:614–618. [PubMed: 22133988]

Pesaresi M, Maschi O, Giatti S, Garcia-Segura LM, Caruso D, Melcangi RC. Sex differences in neuroactive steroid levels in the nervous system of diabetic and non-diabetic rats. Horm Behav. 2010; 57:46–55. [PubMed: 19422828]

Ritch, R. Glaucoma. In: Silverstone, B.Lang, MA.Rosenthal, BP., Faye, EE., editors. Vision Impairment and Vision Rehabilitation. Oxford University Press, Inc; New York: 2000. p. 53-81.

Rone MB, Fan J, Papadopoulos V. Cholesterol transport in steroid biosynthesis: role of protein-protein interactions and implications in disease states. Biochim Biophys Acta. 2009; 1791:646–658. [PubMed: 19286473]

Rupprecht R, Rammes G, Eser D, Baghai TC, Schüle C, Nothdurfter C, Troxler T, Gentsch C, Kalkman HO, Chaperon F, Uzunov V, McAllister KH, Bertaina-Anglade V, La Rochelle CD, Tuerck D, Floesser A, Kiese B, Schumacher M, Landgraf R, Holsboer F, Kucher K. Translocator protein (18 kD) as target for anxiolytics without benzodiazepine-like side effects. Science. 2009; 325:490–493. [PubMed: 19541954]

Rupprecht R, Papadopoulos V, Rammes G, Baghai TC, Fan J, Akula N, Groyer G, Adams D, Schumacher M. Translocator protein (18 kDa) (TSPO) as a therapeutic target for neurological and psychiatric disorders. Nature Reviews Drug Discovery. 2010; 9:971–988. [PubMed: 21119734]

Seki M, Lipton SA. Targeting excitotoxic/free radical signaling pathways for therapeutic intervention in glaucoma. Prog Brain Res. 2008; 173:495–510. [PubMed: 18929130]

Shany E, Hochhauser E, Halper P, Vidne B, Gavish M, Geller E, Hasharoni A, Barak Y, Yakirevich V. Ro5-4864 has a negative inotropic effect on human atrial muscle strips that is not antagonized by PK11195. Eur J Pharmacol. 1994; 253:231–236. [PubMed: 8200417]

Tham YC, Li X, Wong TY, Quigley HA, Aung T, Cheng CY. Global prevalence of glaucoma and projections of glaucoma burden through 2040: a systematic review and meta-analysis. Ophthalmology. 2014; 121:2081–2090. [PubMed: 24974815]

Thoreson WB, Witkovsky P. Glutamate receptors and circuits in the vertebrate retina. Prog Retin Eye Res. 1999; 18:765–810. [PubMed: 10530751]

Tian G. 17b-(N-tert-butylcarbamoyl)-4-aza-5α-androstan- 1-en-3-one is an active site-directed slow time-dependent inhibitor of human steroid 5α-reductase. Biochemistry. 1994; 33:2291–2296. [PubMed: 8117686]

Tokuda K, O'Dell KA, Izumi Y, Zorumski CF. Midazolam inhibits hippocampal long-term potentiation and learning through dual central and peripheral benzodiazepine receptor activation and neurosteroidogenesis. J Neurosci. 2010; 30:16788–16795. [PubMed: 21159950]

Turner MR, Cagnin A, Turkheimer FE, Miller CC, Shaw CE, Brooks DJ, Leigh PN, Banati RB. Evidence of widespread cerebral microglial activation in amyotrophic lateral sclerosis: an [11C] (R)-PK11195 positron emission tomography study. Neurobiol. 2004; 15:601–609.

Veenman L, Papadopoulos V, Gavish M. Channel functions of the 18 kDa translocator protein (TSPO): regulation of apoptosis and steroidogenesis as part of the host defense response. Cur Pharm Des. 2007; 13:2385–2405.

Veiga S, Azcoitia I, Garcia-Segura LM. Ro5-4864, a peripheral benzodiazepine receptor ligand, reduces reactive gliosis and protects hippocampal hilar neurons from kainic acid excitotoxicity. J Neurosci Res. 2005; 80:129–137. [PubMed: 15696538]

Vowinckel E, Reutens D, Becher B, Verge G, Evans A, Owens T, Antel JP. PK11195 binding to the peripheral benzodiazepine receptor as a marker of microglia activation in multiple sclerosis and experimental autoimmune encephalomyelitis. J Neurosci Res. 1997; 50:345–353. [PubMed: 9373043]

Wang M, Wang X, Ma L, Ma W, Rodriguez IR, Fariss RN, Wong WT. Macroglia-microglia interactions via TSPO signaling regulates microglial activation in the mouse retina. J Neurosci. 2014; 34:3793–3806. [PubMed: 24599476]

Weir CJ, Ling AT, Belelli D, Wildsmith JA, Peters JA, Lambert JJ. The interaction of anaesthetic steroids with recombinant glycine and $GABA_A$ receptors. Br J Anaesth. 2004; 92:704–711. [PubMed: 15033889]

Yang XL. Characterization of receptors for glutamate and GABA in retinal neurons. Prog Neurobiol. 2004; 73:127–150. [PubMed: 15201037]

Yasuno F, Ota M, Kosaka J, Ito H, Higuchi M, Doronbekov TK, Nozaki S, Fujimura Y, Koeda M, Asada T, Suhara T. Increased binding of peripheral benzodiazepine receptor in Alzheimer's disease measured by positron emission tomography with [11C]DAA1106. Biol Psychiatry. 2008; 64:835–841. [PubMed: 18514164]

Yawno T, Hirst JJ, Castillo-Melendez M, Walker DW. Role of neurosteroids in regulating cell death and proliferation in the late gestation fetal brain. Neuroscience. 2009; 163:838–847. [PubMed: 19591903]

Zorumski CF, Paul SM, Izumi Y, Covey DF, Mennerick S. Neurosteroids, stress and depression: potential therapeutic opportunities. Neurosci Biobehav Rev. 2013; 37:109–122. [PubMed: 23085210]

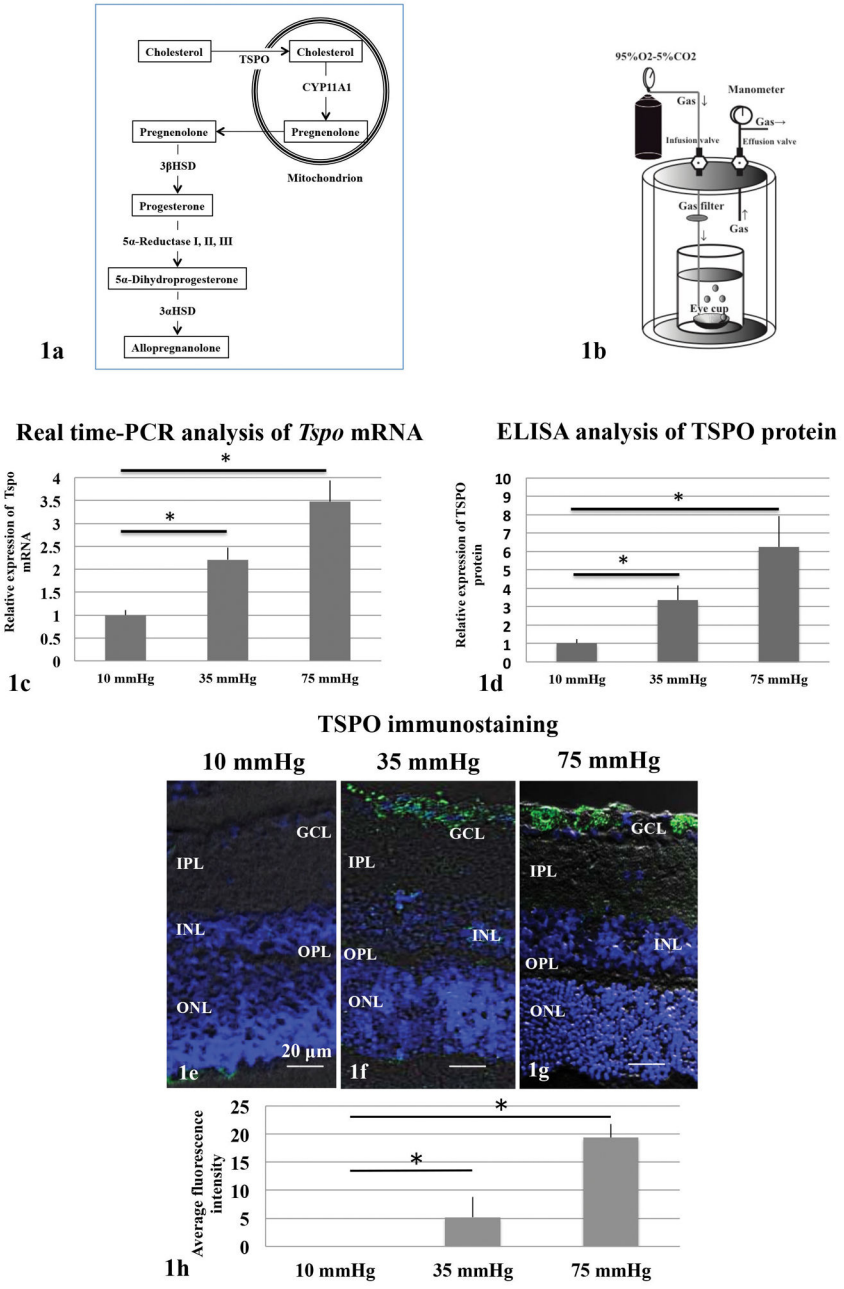


**Fig. 1.**

**a.** The diagram depicts key steps and enzymes involved in the synthesis of AlloP from cholesterol. This scheme is modified from Fig. 3 in the manuscript by Zorumski et al. (2013). **b.** The closed pressure-loading system. Rat *ex vivo* eye cup preparations were placed at the bottom of a 100 mL glass beaker filled with aCSF. The beaker was set at the bottom of an acrylic pressure chamber. A 95% $O_2$–5% $CO_2$ gas mixture was delivered through an infusion valve via disposable plastic tubing that terminated 1 cm above the bottom of the cylinder. Eyecups were incubated at 30°C for 24 hours. Pressure was adjusted to 10 mmHg, 35 mmHg and 75 mmHg by a control dial on the effusion valve. Atriol, MK801, PK11195,

and dutasteride were added to the aCSF buffer during some experiments. **c.** Quantitative real-time RT-PCR analysis of *tspo* mRNA. *Tspo* mRNA expression increased in a pressure-dependent manner and was significantly upregulated at 35 mmHg and 75 mmHg compared to 10 mm Hg. *p<0.05. **d.** Protein levels of TSPO in the pressure-loaded retinas were measured with ELISA. TSPO level significantly increased at 35 mmHg and 75 mmHg compared to 10 mmHg. *p<0.05. **e–g.** Immunofluorescent localization of TSPO (green; FITC) by confocal microscopy. Merge of differential interference contrast images and fluorescence images using DAPI and an antibody against TSPO. **e.** TSPO immunostaining at 10 mmHg. Fluorescence was minimal in a retina incubated at 10 mmHg. **f.** TSPO immunostaining at 35 mmHg. The retina showed marginal changes in fluorescence in the GCL. **g.** TSPO immunostaining at 75 mmHg. Positive immunofluorescence of TSPO was observed in the GCL at 75 mmHg. Fig. 1e–1g are at the same magnification. Scale bars, 20 μm. **h.** Summary of TSO fluorescence intensity (arbitrary units) as mean ± SEM. *p<0.05

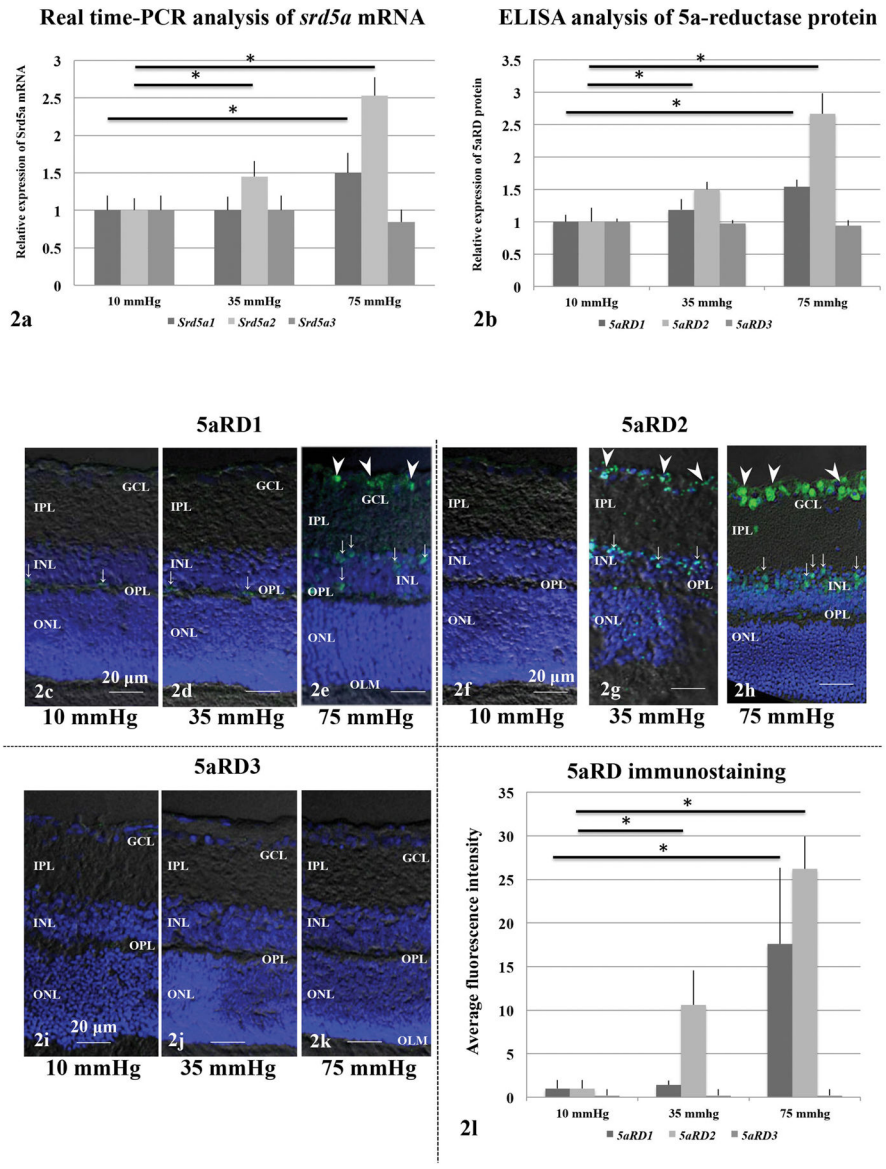


**Fig. 2.**

**a.** Quantitative real-time RT-PCR analysis of *srd5a* mRNA. Expression of *srd5a1* mRNA showed no remarkable changes at 35 mmHg, but significantly increased at 75 mmHg (*p<0.05) compared to 10 mmHg. *Srd5a2* mRNA was significantly increased at 35 mmHg (*p<0.05) and 75 mmHg (*p<0.05) compared to control pressure (10 mmHg). *Srd5a3* mRNA showed no remarkable changes at 35 mmHg and 75 mmHg compared to 10 mmHg. **b.** Protein levels of 5aRD1, 5aRD2 and 5aRD3 in pressure-loaded retinas. Protein levels were measured with ELISA. 5aRD1 level showed no remarkable changes at 35 mmHg, but significantly increased at 75 mmHg (*p<0.05) compared to 10 mmHg. Protein levels of 5aRD2 significantly increased at 35 mmHg (p<0.05) and 75 mmHg (p<0.05) compared to 10 mmHg. 5aRD3 level showed no changes at 35 mmHg and 75 mmHg compared to 10 mmHg. **c–k.** Immunofluorescent localization of 5α-reductase (5aRD) (green; FITC) by confocal microscopy. Merge of differential interference contrast images and fluorescence

images using DAPI and an antibody against 5aRD. **c–e.** 5aRD1 immunostaining at each pressure. Fluorescence was minimal in a retina incubated at 10 mmHg (**c**) and 35 mmHg (**d**), but significantly increased in GCL (arrowheads) and INL (arrows) at 75 mmHg (**e**). **f–h.** 5aRD2 immunostaining in a retina incubated at each pressure. At 10 mmHg, there was minimal fluorescence in the retina (**f**). At 35 mmHg, increased reaction was detected in the GCL (arrowheads) and INL (arrows) (**g**). Positive immunofluorescence was observed in the GCL and INL at 75 mmHg (**h**). Arrowheads and arrows indicate positive fluorescence in the GCL and INL, respectively. **i–k.** 5aRD3 immunostaining at each pressure. Fluorescence was weak in retinas incubated at 10 mmHg (**i**), 35 mmHg (**j**), and 75 mmHg (**k**). Fig. 2c–2k are at the same magnification. Scale bars, 20 μm. **l**. Summary of immunofluorescence intensity by anti-5aRD antibodies. *$p<0.05$.

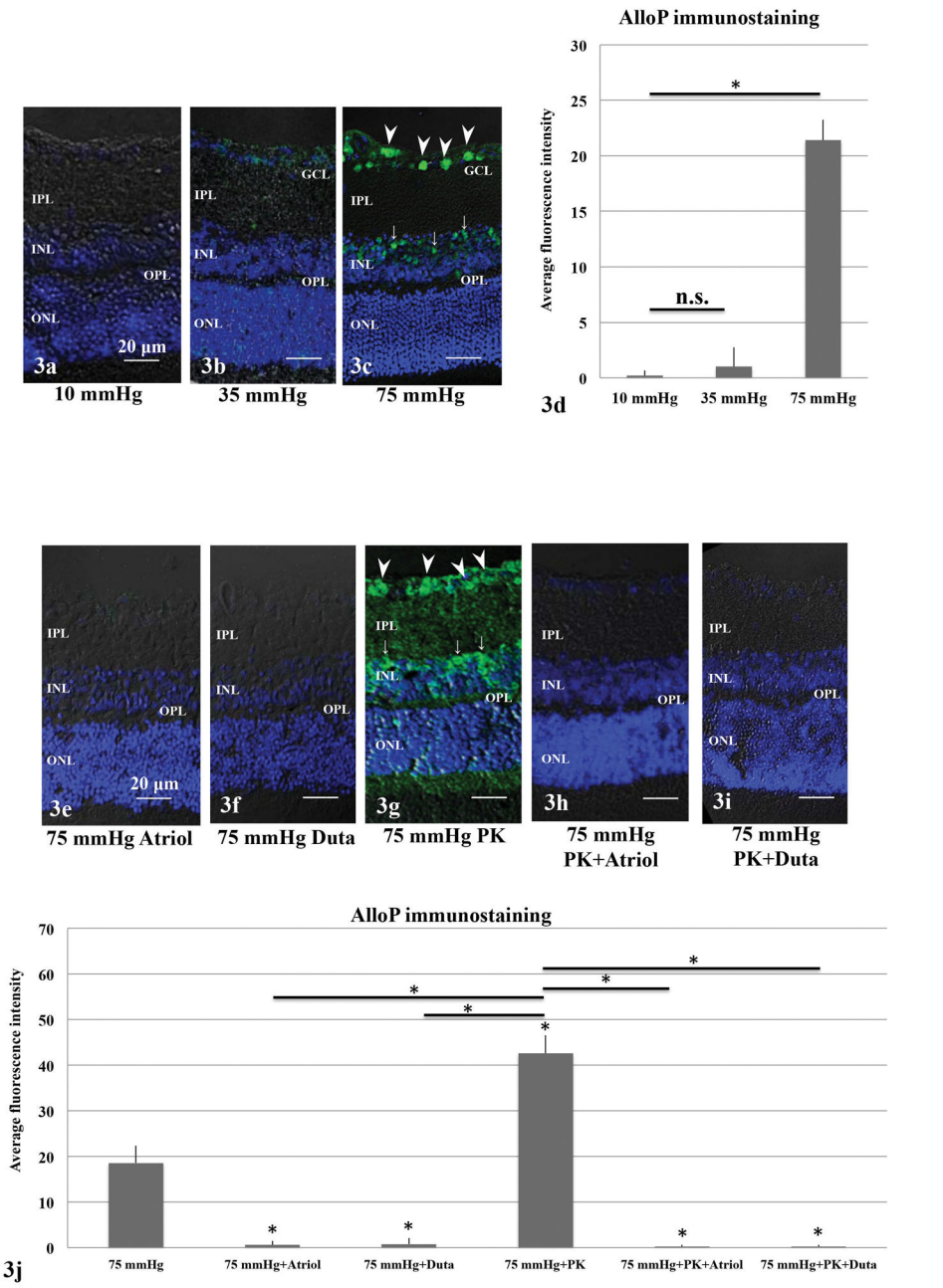


**Fig. 3.**

Immunofluorescent localization of AlloP (green; FITC) by confocal microscopy. **a–c.** AlloP immunostaining at each pressure. **a.** AlloP immunostaining was minimal in a retina incubated at 10 mm Hg. **b.** At 35 mmHg, the retina showed marginal changes in fluorescence in the GCL. **c.** Positive immunofluorescence was observed mainly in the GCL and the INL at 75 mmHg. Arrowheads and arrows indicate immunofluorescence in the GCL and INL, respectively. **d.** Summary of pressure-dependent immunofluorescence by anti-AlloP antibody. Statistical differences compared to controls incubated at 10 mmHg were analyzed using Dunnett's multiple comparison test. *$p<0.05$. **e and f**. Effects of atriol and

dutastreride on AlloP staining. Administration of atriol almost completely eliminated the fluorescence observed at 75 mmHg (**e**), while marginal fluorescence was detected in the vicinity of the RGC in the retina incubated with 1 μM dutasteride at 75 mmHg (**f**). **g.** Administration of PK11195 significantly increased AlloP fluorescence in the GCL (arrowheads), INL (arrows) and ONL at 75 mmHg. **h and i.** Enhancement of AlloP fluorescence by PK11195 was inhibited by atriol (**h**) and dutasteride (**i**). **j.** Summary of immunofluorescence by anti-AlloP antibody. Statistical differences were analyzed using Tukey's multiple comparison test. Bars with asterisks are significantly different from controls incubated with aCSF at 75 mmHg (*$p<0.05$).

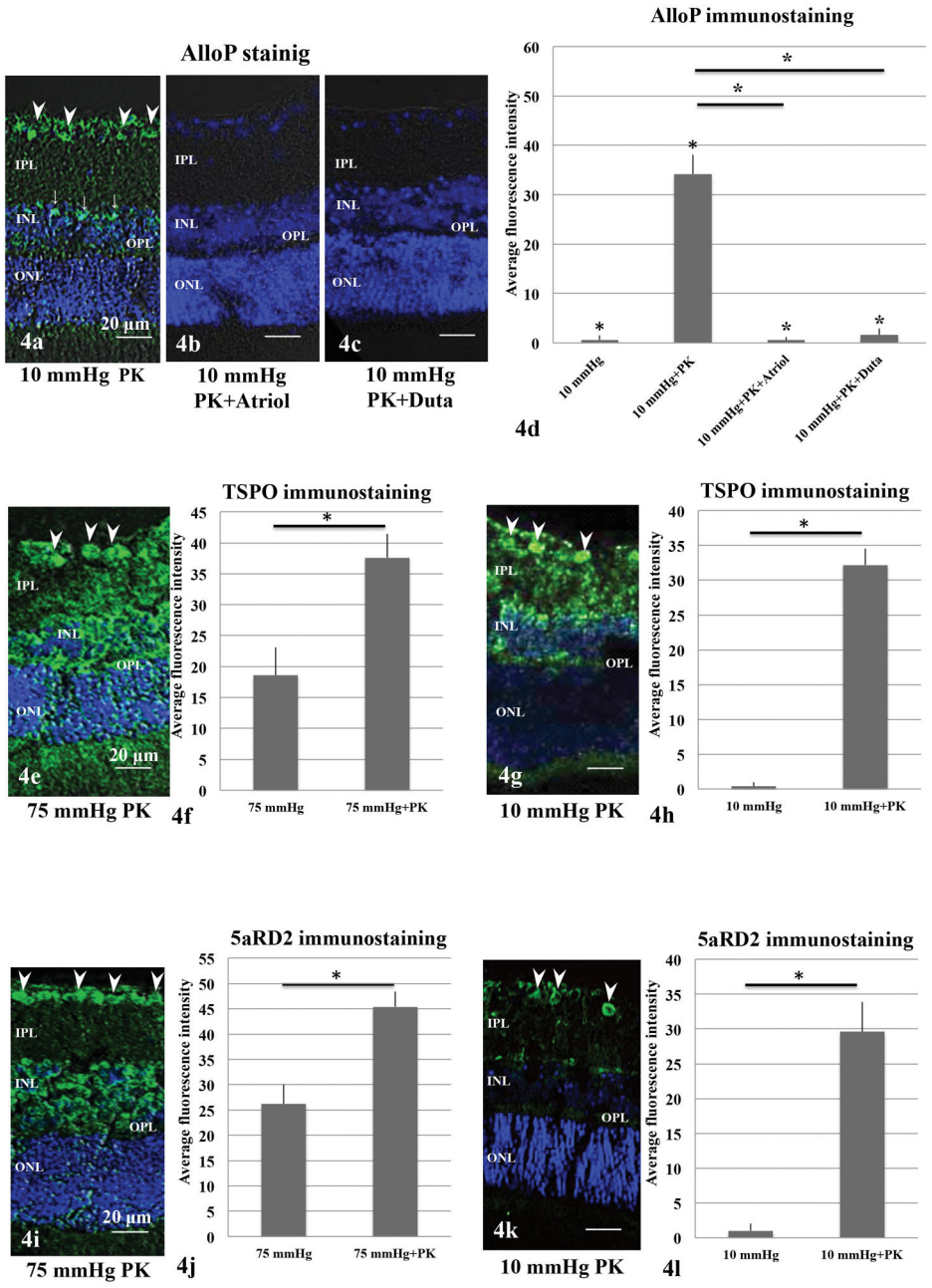


**Fig. 4.**

**a–c.** Immunofluorescent localization of AlloP (green; FITC) by confocal microscopy. **a.** Effects of PK11195 on immunostaining. Administration of PK11195 significantly increased fluorescence of AlloP in the GCL (arrowheads), IPL, INL (arrows) and ONL at 10 mmHg. **b and c.** Administration of atriol (**b**) and dutasteride (**c**) significantly decreased fluorescence in the presence of PK11195 at 10 mmHg. **a–c** are at the same magnification. Scale bars, 20 µm. **d.** Summary of immunofluorescence by anti-AlloP antibody. Statistical differences were analyzed using Tukey's multiple comparison test. Bars with asterisks are significantly different from controls incubated with aCSF at 10 mmHg (*$p<0.05$). **e–h.** Effects of

PK11195 on the immunofluorescence of TSPO at 75 mmHg (**e**) and 10 mmHg (**g**). Administration of PK11195 significantly enhanced immunofluorescence of TSPO in the GCL, IPL, INL, OPL, ONL, and OLM at 75 mmHg (**e and f**). PK11195 also increased immunofluorescence of TSPO in the GCL, IPL, INL, and OPL at 10 mmHg (**g and h**). Arrowheads indicate GCL. *p<0.05**. i–l.** Effects of PK11195 on the immunofluorescence of 5aRD2 at 75 mmHg (**i**) and 10 mmHg (**k**). Administration of PK11195 significantly enhanced immunofluorescence of 5aRD2 in the GCL, INL, ONL, and OLM at 75 mmHg (**i and j**). PK11195 also increased immunofluorescence of 5aRD2 in the GCL and IPL at 10 mmHg (**k and l**). Arrowheads indicate GCL. *p<0.05.

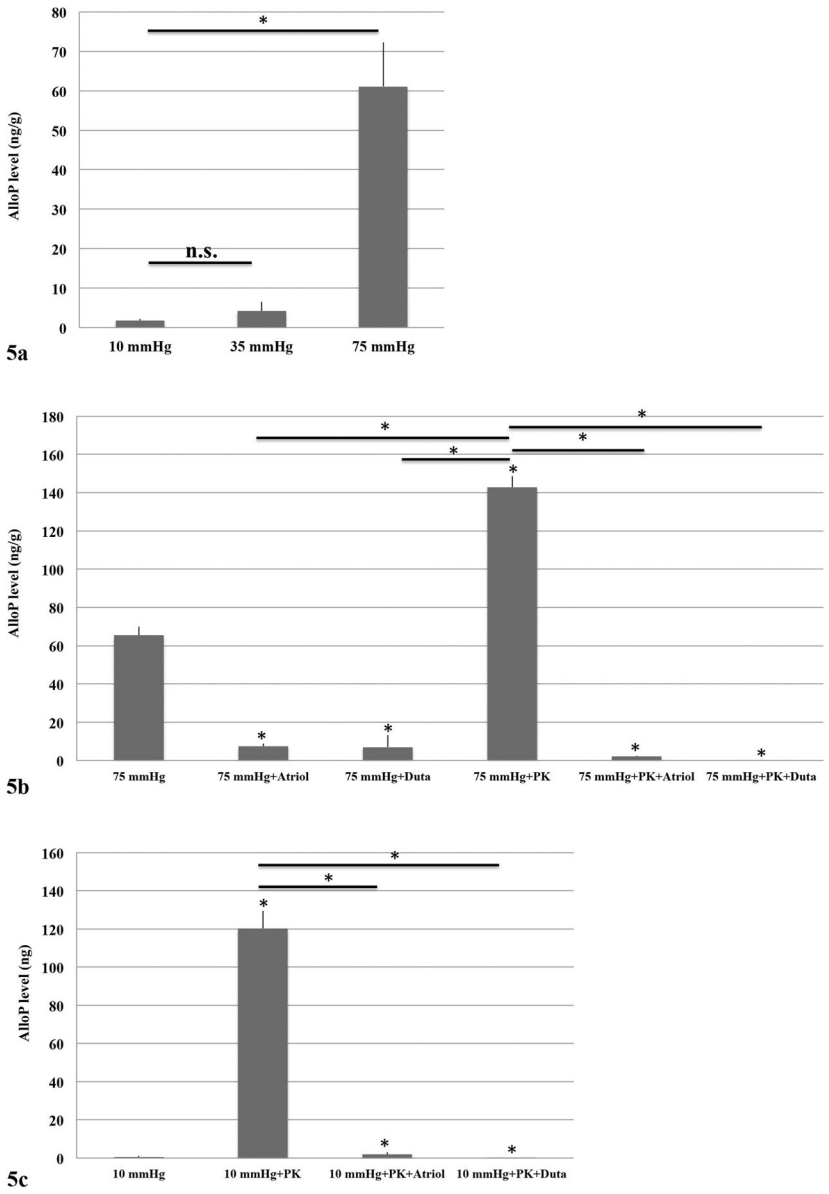


**Fig. 5.**

Measurement of AlloP in retinal extracts using LC-MS/MS. **a.** AlloP levels significantly increased at 75 mmHg compared to control pressure (10 mmHg) by Dunnett's test. **b.** At 75 mmHg, administration of 1 μM atriol or 1 μM dutasteride (Duta) significantly depressed the increase of AlloP compared to retinas incubated in aCSF. Administration of 50 μM PK11195 (PK) significantly increased AlloP levels at 75 mmHg compared to retinas incubated without PK at 75 mmHg. Administration of 1 μM atriol or 1 μM Duta significantly inhibited the AlloP increase at 75 mmHg. Statistical differences were analyzed using Tukey's multiple comparison test. Bars with asterisks are significantly different from controls incubated with aCSF at 75 mmHg (*$p<0.05$). **c.** Administration of 50 μM PK also increased AlloP levels at 10 mmHg compared to retinas incubated without PK at 10 mmHg. Administration of 1 μM atriol or 1 μM Duta significantly dampened the AlloP increase by PK. Statistical differences

were analyzed using Tukey's multiple comparison test. Bars with asterisks are significantly different from controls incubated with aCSF at 10 mmHg (*$p<0.05$).

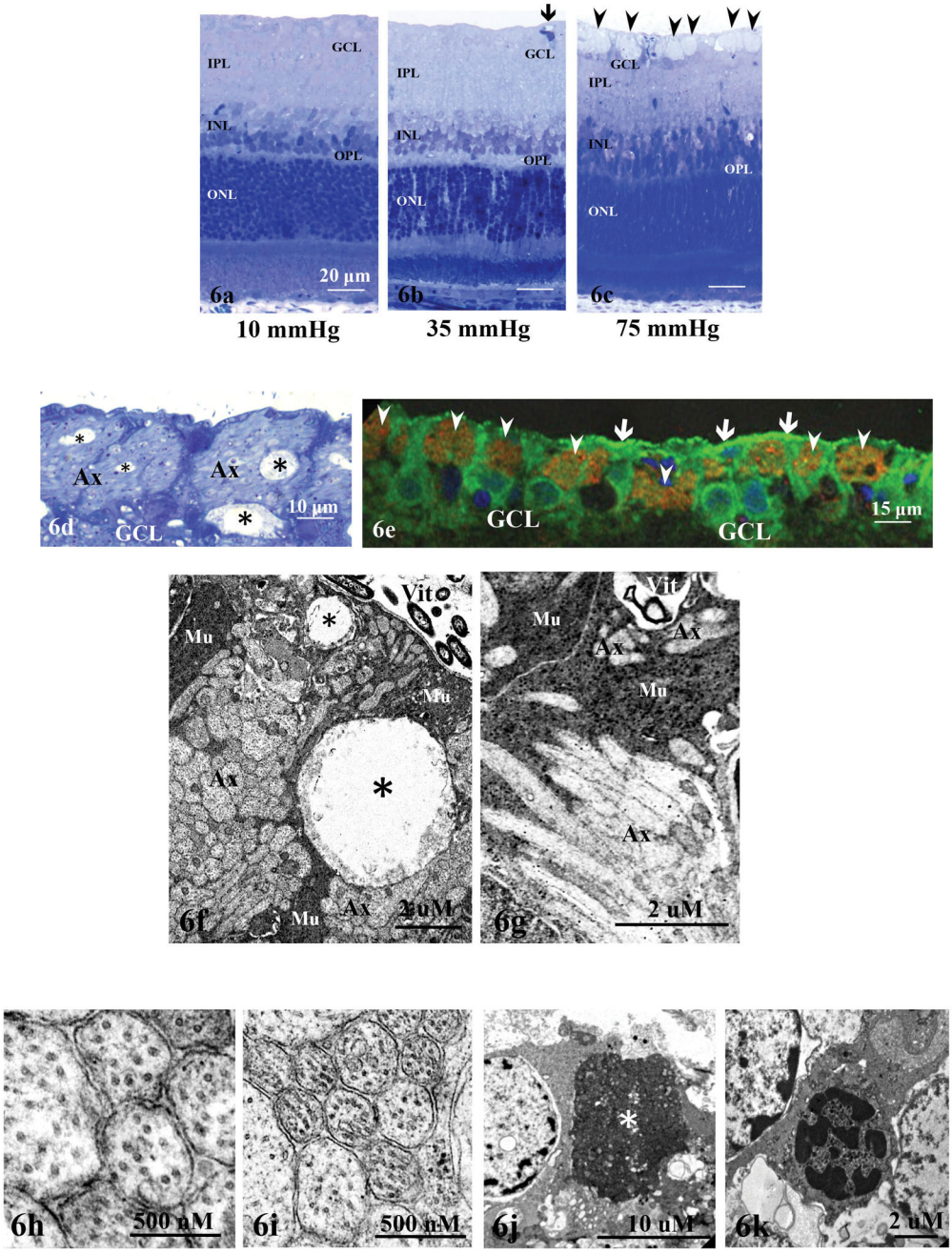


**Fig. 6.**

**a–d**. Light micrographs of pressure-dependent changes in the retina. In retinas incubated at 10 mmHg (**a**) and 35 mmHg (**b**), no major changes were detected. Arrow indicates blood vessel. Prominent axonal swelling of the RGCs (arrowheads) was observed in a retina incubated at 75 mmHg (**c**). **a–c** are at the same magnification. Scale bars, 20 µm. **d.** Enlargement of the axonal swelling (Ax) in the retina after pressure loading at 75 mmHg. Asterisks indicate vacuoles in the NFL. GCL; ganglion cell layer. **e.** Immunohistochemistry revealed that swollen RGC axons (arrowheads) were specifically labeled with anti-Thy 1.1

antibody (red; RGC axonal marker), but not with anti-GFAP antibody (green; glial marker). Arrows indicate the end feet of Müller cells labeled with anti-GFAP antibody. **f–k.** Electron micrographs of the NFL and GCL after pressure elevation (75 mmHg). **f and g.** Note the transversely (**f**) and longitudinally (**g**) sectioned swollen axons (Ax) at 75 mmHg. Asterisks indicate vacuole formation in the NFL. Mu; Müller cell, Vit; vitreous cavity. **h and i.** Electron microscopy revealed substantial swelling of axons after exposure to high pressure (**h**; 75 mm Hg) compared with control axons in a retina incubated at 10 mm Hg (**i**). **h and i** are at the same magnification. Scale bars, 500 nm. **j and k.** Elevated pressure also increased the number of degenerated cells (**j**) or apoptotic cells with chromatin condensation at the edge of the nucleus in the GCL (**k**).

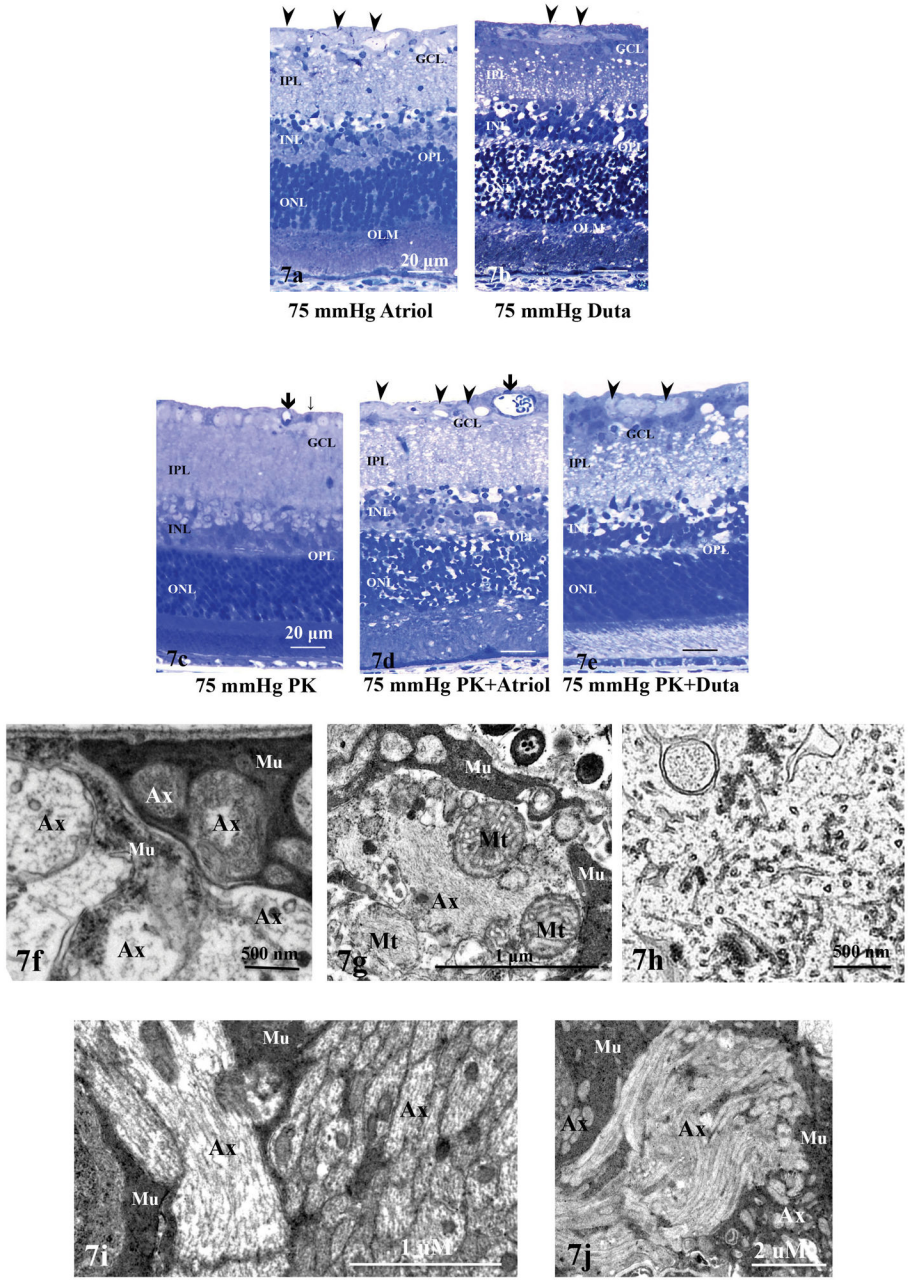


**Fig. 7.**

Light micrographs of retinas incubated at 75 mmHg. **a and b.** Treatment with 1 μM atriol (a) or 1 μM dutasteride (b, Duta) induced excitotoxic changes characterized by bull's eye formation in the INL and edematous changes in the IPL along with axonal swelling in the NFL (arrowheads) in retinas at 75 mmHg. Duta also induced damage in the ONL. **c.** Axonal swelling in the NFL induced by pressure elevation was inhibited in a retina incubated with 50 μM PK11195 at 75 mmHg. Bold arrow and thin arrow indicate blood capillary and nuclear pyknosis in the GCL, respectively. **d.** Administration of 1 μM atriol induced retinal degeneration characterized by bull's eye formation in the INL, edema in the IPL and axonal

swelling (arrowheads) in a retina treated with 50 μM PK11195 (PK) at 75 mmHg. The ONL was also damaged. Bold arrow indicates blood capillary. **e.** Administration of 1 μM Duta induced excitotoxic retinal degeneration and axonal swelling (arrowheads) in a retina treated with 50 μM PK at 75 mmHg. **a–e** are at the same magnification. Scale bars, 20 μm. **f–j.** Electron micrographs of the NFL. **f.** Combination of high pressure and atriol (1 μM) resulted in degeneration of swollen axons (Ax). **g and h.** Combination of high pressure and dutasteride (1 μM) resulted in axonal swelling (Ax) with degenerated cell organelles (Mt; swollen mitochondria) (**g**) and electron-dense materials in the swollen axons (**h**). The combination of high pressure and 1 μM atriol (**i**) or 1 μM Duta (**j**) also induced marked axonal swelling (Ax) in the presence of PK11195. Mu; Müller cells.

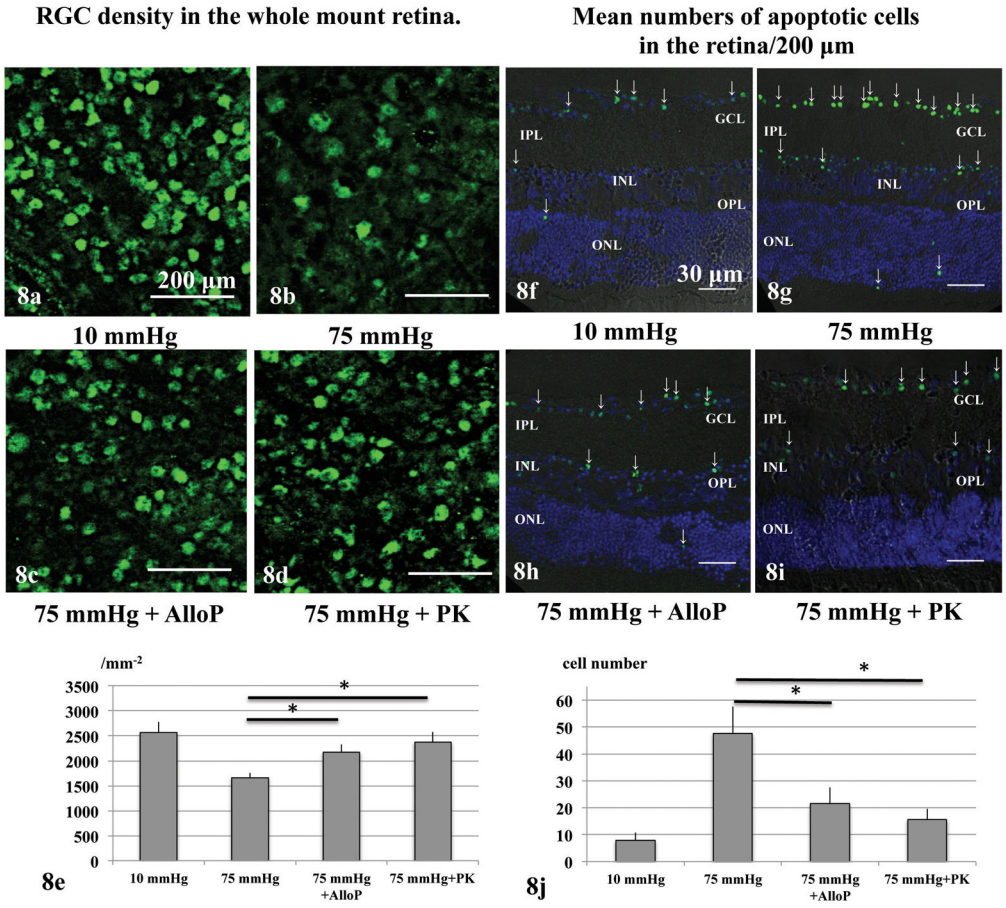


**Fig. 8.**

**a–d**. RGC survival using the RGC marker (NeuN) in the whole mount retina. **a.** Confocal images of NeuN-labeled RGCs in a control eye incubated at 10 mmHg. **b.** The density of NeuN-positive RGCs was reduced at 75 mmHg compared to control pressure (10 mmHg). **c and d.** Administration of AlloP (1 µM) (**c**) or PK11195 (50 µM) (**d**) enhanced RGC survival under hyperbaric conditions. **a–d** are at the same magnification. Scale bars, 200 µm. **e.** The graph presents the number of NeuN-positive cells in the whole mount retina under each experimental condition. Quantitative analysis confirmed that administration of AlloP (1 µM) or PK11195 (50 µM) promoted significant RGC survival compared with control retina incubated in aCSF at 75 mmHg. The densities of RGC soma in retinas incubated in aCSF at 10 mmHg are shown as reference. *$p<0.05$. **f–i.** Visualization of apoptotic cells by fluorescence microscopy. Merge of differential interference contrast images and fluorescence images using DAPI and TUNEL-fluorescent staining of retinas incubated at 10 mmHg (**f**), and 75 mmHg (**g**). **f.** At 10 mmHg, a few TUNEL-positive cells (fine arrows) can be observed within the GCL, INL, and ONL. **g.** At 75 mmHg, there was a marked increase of TUNEL-positive cells in the GCL as well as some cells in the INL and ONL. **h and i.** Administration of 1 µM AlloP (l) or 50 µM PK11195 (m) significantly decreased a number of TUNEL-positive cells at 75 mmHg. **f–i** are at the same magnification. Scale bars, 30 µm. **j.** The graph presents the number of TUNEL-positive RGCs per 200 µm of the retinal

section. Quantitative analysis confirmed that administration of AlloP (1 μM) or PK11195 (50 μM) promoted significant inhibition of apoptotic cells compared with control retina incubated in aCSF at 75 mmHg. The number of apoptotic cells in retinas incubated in aCSF at 10 mmHg is shown as a reference point. *$p<0.05$.

## Table 1

The list of the oligonucleotides used for quantitative real-time RT-PCR with GenBank accession number, forward and reverse primer sequences, and product size.

| Gene (Protein) | GenBank accession number | Forward (F) and reverse (R) primer sequences | Product size (bp) |
|---|---|---|---|
| ***Tspo*** **(TSPO)** | NM_012515.2 | F: TACACTGGTCAGCTGGCTCTGAA<br>R: ACAAGCATGAGGTCCACCAAAG | 93 |
| ***Srd5a1*** **(5aRD1)** | NM_017070.3 | F: TGCACTGTTCACACTCAGCACAC<br>R: GCAACAGCGCTAACAGAGCACTA | 138 |
| ***Srd5a2*** **(5aRD2)** | NM_022711.4 | F: GGGACCCTGATCCTGTGCTTA<br>R: GGAACTCCCGACGACACACT | 73 |
| ***Srd5a3*** **(5aRD3)** | NM_001013990.1 | F: GTACTGAGCCAAGTGCCCATGA<br>R: ATGTGGAACCACCGAGCTTGTAG | 83 |
| ***Gapdh*** **(GAPDH)** | NM_017008.3 | F: GCCAAAAGGGTCATCATCTCCG<br>R: ACATTGGGGGTAGGAACACGGA | 143 |

## Table 2

Effects of pressure elevation on the NFLT, NDS, and the density of the damaged cells in the GCL. p values were calculated using Dunnett's multiple comparison test.

| Condition (n) | NFLT vs. RT (%)[p] | NDS [p] | Damaged cells in the GCL [p] |
|---|---|---|---|
| **10 mmHg (10)** | 1.3 ± 0.7 [-] | 0.1 ± 0.3 [-] | 0.1 ± 0.3 [-] |
| **35 mmHg (10)** vs. 10 mmHg | 1.4 ± 0.9 [p>0.05] | 0.1 ± 0.3 [p>0.05] | 0.3 ± 0.5 [p>0.05] |
| **75 mmHg (10)** vs. 10 mmHg | 9.6 ± 1.7 [*p<0.05] | 1.1 ± 0.3 [*p<0.05] | 16.2 ± 5.0 [*p<0.05] |

## Table 3

Effects of pressure elevation and administration of atriol, MK801, or AlloP on the NFLT, NDS, and the density of the damaged cells in the GCL. p values were calculated using Dunnett's multiple comparison test.

| Condition (n) | NFLT vs. RT (%) [p] | NDS [p] | Damaged cells in the GCL [p] |
|---|---|---|---|
| **75 mmHg+1 μM Atriol (10)** vs. 75 mmHg | 7.8 ± 1.0 [p>0.05] | 3.6 ± 0.5 [*p<0.05] | 55.7 ± 11.2 [*p<0.05] |
| **75 mmHg+1 μM Dutasteride (10)** vs. 75 mmHg | 7.6 ± 1.6 [p>0.05] | 3.4 ± 0.7 [*p<0.05] | 56.4 ± 17.1 [*p<0.05] |
| **75 mmHg + 50 μM PK11195 (10)** vs. 75 mmHg | 0.9 ± 0.9 [*p<0.05] | 0.1 ± 0.3 [*p<0.05] | 2.2 ± 2.2 [*p<0.05] |
| **75 mmHg + 50 μM PK11195 +1 μM Atriol (10)** vs. 75 mmHg | 4.1 ± 3.6 [*p>0.05] | 3.3 ± 0.5 [*p<0.05] | 33.4 ± 18.4 [*p<0.05] |
| **75 mmHg + 50 μM PK11195 +1 μM Dutasteride (10)** vs. 75 mmHg | 4.4± 2.6 [p>0.05] | 3.6± 0.5 [*p<0.05] | 52.5 ± 12.7 [*p<0.05] |